Characterising Magmatic Suites in the Western Gawler Craton: Geochemical and Geochronological Constraints

Thesis submitted in accordance with the requirements of the University of Adelaide for an Honours Degree in Geology

Jack Dawson
November 2016

THE UNIVERSITY of ADELAIDE

ABSTRACT

The western Gawler Craton is host to two uncharacterized Paleoproterozoic magmatic suites that had previously been mapped with no geochronological or geochemical constraints. There needed to be a better understanding of the magmatic suites in order to constrain the magmatic and tectonic evolution of the understudied area. This study provides insight to the known extent of the two magmatic suites using field relationships in conjunction with petrography, geochemistry and geochronological constraints, which has implications for the geological setting and tectonic evolution during the Paleoproterozoic. U-Pb dating of an unnamed granite suite yielded ages of 1694.5±6 Ma and is classified geochemically as weakly peraluminous and high K-calc-alkalic. Age and geochemistry closely resembles that of the Tunkillia Suite granitoids and is proposed as an equivalent. Further isotopic constraints implicate a syn- late tectonic setting during the cessation of the Kimban Orogeny. U-Pb dating of a gabbroic suite revealed an age of 1712.4±6 Ma which is comparable in age and isotopic nature to mafic members of the newly proposed Peter Pan SuperSuite.

Keywords: Gawler Craton, Geochemistry, Tectonic setting, Tunkillia Suite, Peter Pan SuperSuite, Geochronology

TABLE OF CONTENTS

LIST OF FIGURES AND TABLES

INTRODUCTION

A significant percentage of the continental crust is composed of granitoids, therefore they play an important role in shaping the geochemical and thermal structure of the crust (Sandiford et al., 2002). The comprehensive study and characterisation of the petrogenesis of granitoids provides vital insights into the tectonic history of crustal evolution. Throughout the Gawler Craton, Precambrian magmatic rocks are generally poorly exposed, being largely obscured by younger sedimentary and metasedimentary sequences. Only an estimated 1% of these suites can be observed in outcrop. This hampers the identification of geological, structural and tectonic relationships (Teasdale, 1997; McLean and Betts, 2002; Stewart and Betts, 2010a; Payne et al., 2010).

The sedimentary sequences consequently often make it difficult to distinguish geological and lithological connections between magmatic suites. Furthermore, this makes constraining the mechanisms of petrogenesis and tectonic regimes problematic. In order to establish connections between magmatic suites and determine their tectonic settings, a combination of geochemistry and geochronology analysis can be utilised in addition to field observations (Stewart and Betts, 2010a).

Advances in understanding the tectonic evolution in the western Gawler Craton and the characterisation of magmatic suites has been highlighted by two distinctive magmatic suites found in the BARTON, TARCOOLA and TALLARINGA 1:250,000 Map sheet areas, intruding the Christie and Fowler Domains (Figs.1,2). The first is an apparent comagmatic sequence of granite, granodiorite and diorite found scattered throughout BARTON and TARCOOLA. The second is a gabbro-diorite suite located at Lake Anthony in TALLARINGA (Fig.2). Herein they are referred to as the ‘unnamed granites’ and the ‘Lake Anthony gabbros’.

Previously both suites have been loosely incorporated into the 'Lincoln Complex' (Rankin., 1996; Benbow, 1991) a term used to describe a host of undifferentiated granitoids in the Gawler Craton (Webb et al., 1986). The term 'Lincoln Complex' is currently being dismantled in favour more appropriate classifications.

Previous work is exceptionally limited, with much of the information on the unnamed granites and Lake Anthony gabbros coming exclusively from 1:250,000K Map sheet explanatory notes of the TALLARINGA and BARTON areas. Rb-Sr model dating of 'Lincoln Complex' rocks at Lake Ifould are thought to constrain ages of both suites to the late Paleoproterozoic (1667±115 Ma; Rankin, 1996). Comagmatic relationships exhibited by the unnamed granites have been described with an affinity to the I-type granitoids of White and Chappell (1983) and have been interpreted by Rankin (1996) as "co-magmatically injected magmas, derived by fractionation and zoning of a lower crustal I-type magma". The unnamed granites are thought to be closely related or equivalent to the I-type granitoids of the Tunkillia suite described by Ferris, (2004), originating in a post-late tectonic setting (Payne, 2008)

The Lake Anthony gabbros were initially described by Benbow (1991) as "a suite of dioritic and acid igneous intrusives that outcrop as massive, weakly foliated, and fine to medium grained, occurring with granodiorite and adamellite". New findings suggest they are equivalent to mafics in the Peter Pan SuperSuite newly proposed by Wade and McAvaney (2016), which comprise of all felsic suites and minor mafic suites that intruded during the Kimban Orogeny (1730 – 1690 Ma) (Hand et al., 2007).

In this paper we present new data including U-Pb zircon data, whole rock geochemistry and Sm-Nd isotope geochemistry of the unnamed granites and Lake Anthony gabbro from the BARTON and TALLARINGA areas respectively. The samples presented were

obtained directly from limited basement exposures in the western Gawler Craton. We address their petrogenesis and potential relationship to the Tunkillia Suite and Peter Pan SuperSuite mafics based on geochronological and geochemical constraints. We also use this data to place these Paleoproterozoic magmatic rocks into a geological framework in the western Gawler Craton.

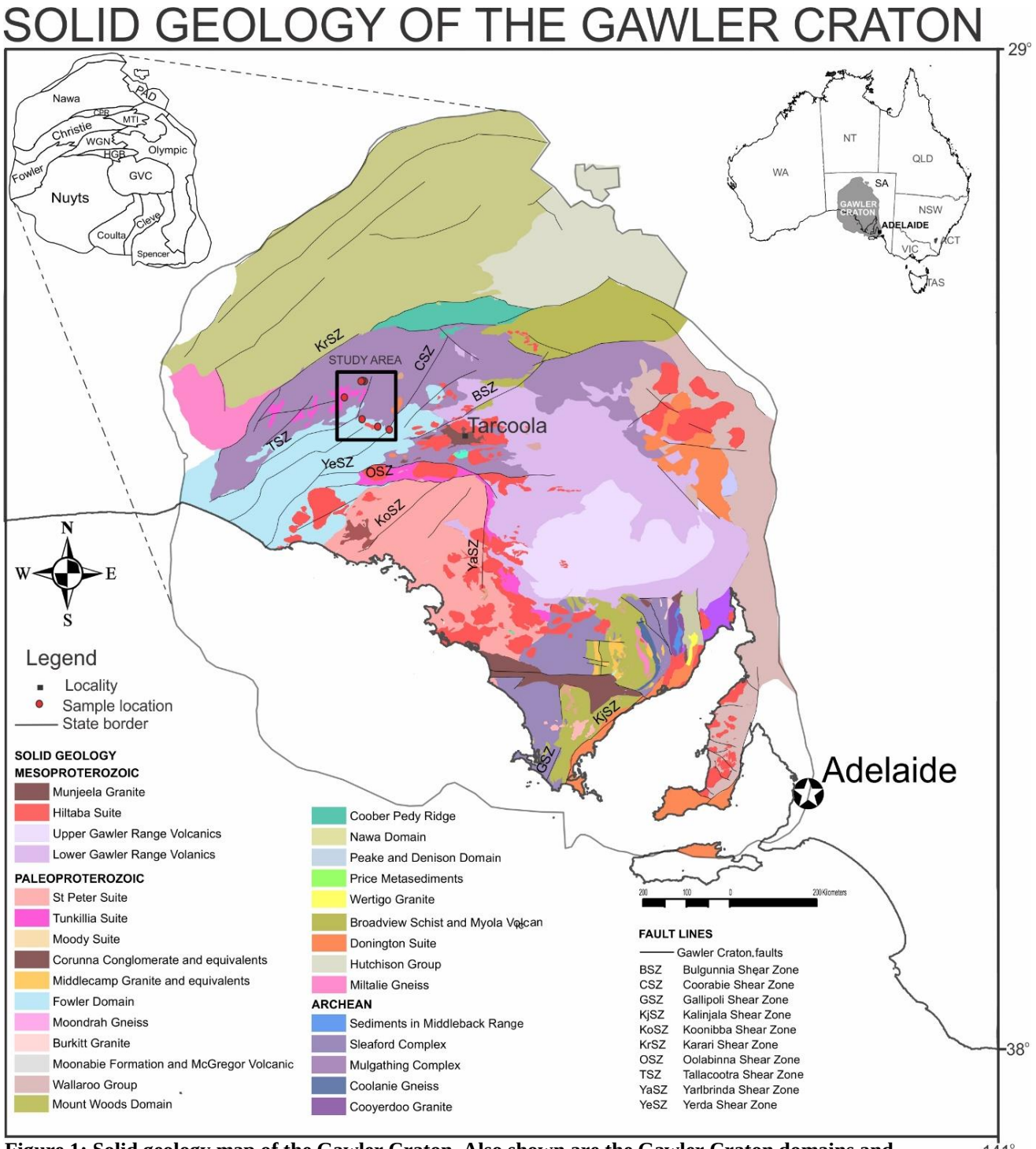

Figure 1: Solid geology map of the Gawler Craton. Also shown are the Gawler Craton domains and faultlines. Area of study is shown as a black square representative of Fig.2. Domains and Solid Geology data was obtained from unpubGSSA. Domain abbreviations; (GVC) Gawler Range Volcanics, (WGN) Wilgena, (PAD) Peak and Denison, (CPR) Coober Pedy Ridge, (MTI) Mt Woods Inlier, (HGB) Harris Greenstone Belt.

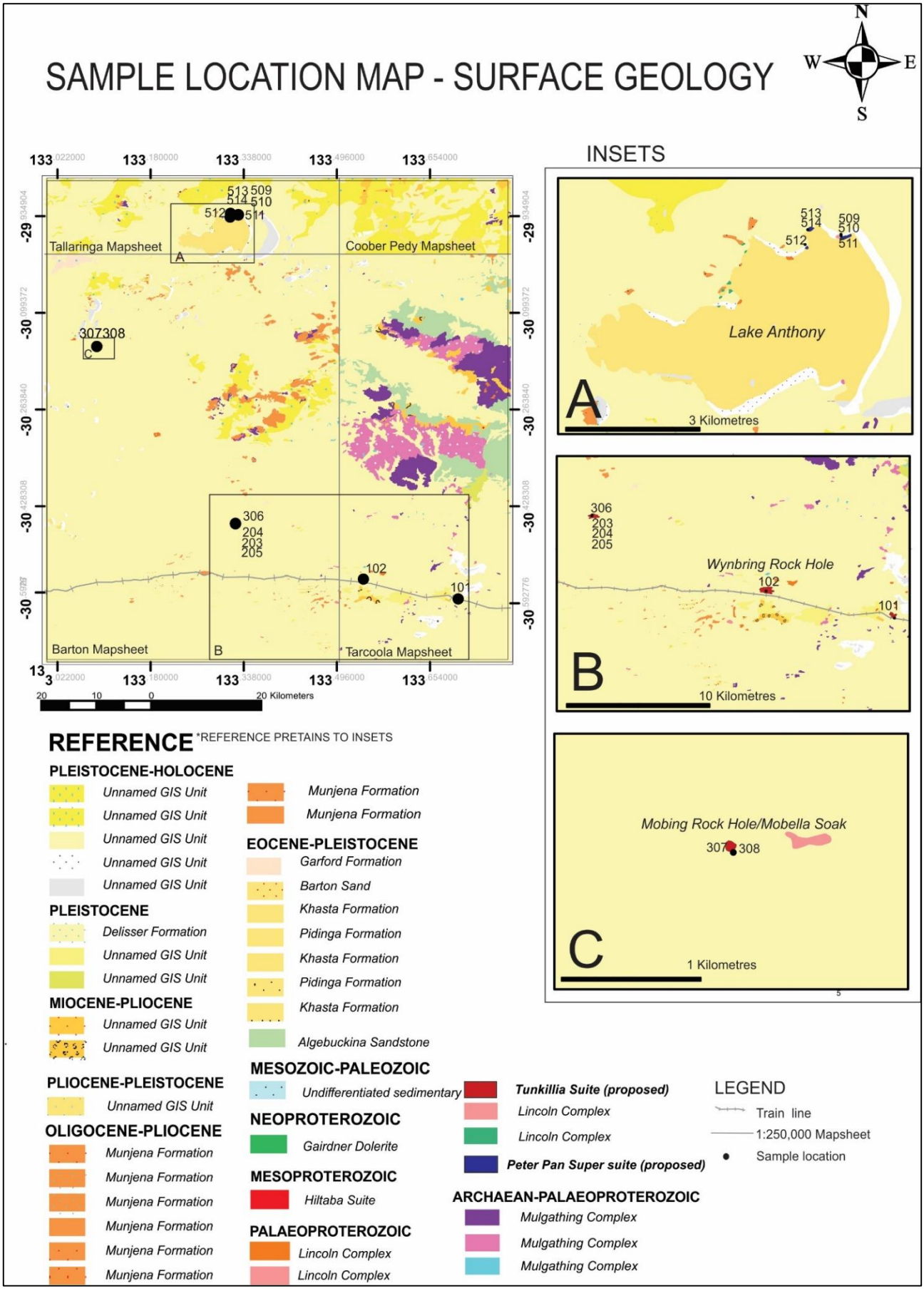

Figure 2: Surface geology map of the study area including insets (A) Lake Anthony, (B) Wynbring Rock Hole and samples near Edoldeh Rock Hole (C) Mobing and Mobella Soak. Polygons of former 'Lincoln Complex units have been changed to proposed Tunkillia Suite (red) and Peter Pan SuperSuite (blue). Data surface geology maps and reference obtained from SARIG.

GEOLOGICAL SETTING

The Gawler Craton is a Mesoarchean-Mesoproterozoic crystalline basement that underlies most of central South Australia (Fig.1) (Fanning et al., 1988; Daly et al., 1998; Ferris et al., 2002; Fraser et al., 2010). It covers an area of ~440,000km^2 and consists of supracrustal rocks that have not been deformed since ~1450 Ma (Daly et al., 1998).

The oldest rocks are Mesoarchean gneisses (~3150 Ma) that have been recently identified on the eastern margin of the Craton (Fraser et al., 2010). The Archean nucleus of the Craton consists of volcanosedimentary rocks (~ 2560 – 2480 Ma) that were deformed and metamorphosed during the Sleaford Orogeny (~2470 – 2410 Ma) (Jagodzinski et al., 2009) producing greenschist to granulite facies metamorphism (Daly and Fanning, 1993). These metamorphosed rocks make up Sleaford Complex in the southern Coulta Domain and the Mulgathing Complex in northern Christie Domain (Fig.1) (Daly et al., 1998; Hand et al., 2007).

Following a period of quiescence (~ 2400-2000 Ma) (Stewart and Betts, 2010) was the Cornian Orogeny, a major tectonic event associated with granulite facies metamorphism (~1850 Ma) (Reid et al., 2008), and coeval with the emplacement of the Donington Suite. Following the Cornian Orogeny was the widespread ~1730 – 1690 Ma Kimban Orogeny (Fanning et al., 2007; Payne et al., 2008), in which the Paleoproterozoic sedimentary rocks overlying the Mulgathing complex were metamorphosed. The Kimban orogeny was largely a transpressional regime, associated with lower amphibolite metamorphism with high T to medium P conditions (Daly et al., 1998). It was accompanied by felsic and minor mafic magmatism, with the emplacement of the Moola Suite (1750 – 1735 Ma), the Pinbong Suite (~1735 – 1700 Ma) (Wade and McAvaney, 2016) and the Moody Suite (~1700 Ma) (Schwarz, 1999). Post Kimban

(1690 – 1670 Ma) orogenic magmatism consists of plutonic and volcanic rock suites, including the emplacement of the Tunkillia Suite granitoids (Ferris, 2004; Payne, 2008) margining the Christie, Wilgena and Nuyts Domains (Fig. 1). The tectonic setting of the Tunkillia suite is debated, however Payne et al. (2008) suggests the Tunkillia formed in a post-late tectonic back arc setting.

Following the Kimban Orogeny is the Ooldean event which occurred from ~1660 – 1630 Ma. This event is recorded in the metapelites of the Moondrah gneiss of the Nawa Domain (Hand et al., 2007). Shortly following is an episode of extensive magmatism by the emplacement with the St Peter Suite at ~1610 Ma (Swain et al. 2008) and Gawler Range Volcanics at ~1590 Ma (Fanning et al., 1988). The Gawler Range Volanics are comagmatic with the voluminous A-type granites of the Hiltaba suite (Fanning et al., 1988) representing a major magmatic event in the Gawler Craton and demonstrates evidence of a back-arc basin for that time (Wade et al., 2006).

The final rock forming period of the Gawler Craton is defined by the Kararan orogeny. The Kararan Orogeny is related to ~1570 – 1540 Ma tectonism and appears to be spatially linked to the Karari fault zone and a series of northeast trending shear zones in the north western Gawler Craton. There appears to be reactivation of shear systems between ~ 1470 and 1450 Ma, however there is no evidence for coeval tectonism at this time (Hand et al., 2007).

Methods

Field work was undertaken from the 17th to the 24th of March in 2016, covering the TARCOOLA, BARTON and TALLARINGA 1:250,000 map sheets (Fig.2). 14 samples were selected for geochronological and geochemical analysis. Three samples were highly weathered or altered and were used for reference only. Fresh samples were obtained and transported back to Adelaide University for analysis.

11 samples were prepared for geochemical analysis. Rocks were prepared using a rock saw and steel crusher and were milled by a tungsten-carbine mill. Whole rock geochemical analysis was performed at Australian Laboratory Services Pty. Ltd (ALS) Major and trace element analysed by inductively coupled plasma mass spectrometry. (ICP-MS). Geochemical results are reported in Table 4.

Three of the samples were selected for zircon U-Pb dating based on lithological similarities. Two unnamed granites samples (307 and 306) and a diorite sample from Lake Anthony (sample 514). Zircon grains sizes between 79 and 400 microns were obtained by sieving followed by separation of light and magnetic portions by hand magnets and heavy liquids methods (Lithium heteropolytungstates). Individual zircon grains were handpicked using an optical microscope before being mounted onto epoxy resin blocks. Blocks were polished and carbon coated for cathodoluminescence imaging (CL). Which was undertaken at Adelaide Microscopy, University of Adelaide, using the Phillips XL-20 Scanning electron Microscope (SEM) with a Gaton CL detector. U–Pb zircon and monazite geochronology analyses was obtained using a RESOchron ASI M50 193 nm Excimer Laser in a helium ablation atmosphere, coupled to an ICP-MS. U–Pb fractionation was corrected using the GJ zircon standard. The $^{207}Pb/^{206}Pb$

grain ages were used, and cores larger than 30 microns were targeted. Accuracy was checked using the Plesovice zircon standard (Sláma et al. 2008) and data was processed using the 'iolite' program. A cut off of <10% concordancy was used for the unnamed granites and <5% for the Lake Anthony diorite.

Five samples were analysed for Sm – Nd analysis which comprised of two unnamed granites and three Lake Anthony gabbros. Methods used follow that of Wade et al. (2006). Sm and Nd was measured by thermal ionization mass spectrometry on a Finnigan MAT 262 thermal ionisation mass spectrometer (TIMS). Sm was analysed on Finnigan Mat 162 and Nd on Mat 262.

11 of the samples had thin sections produced by Continental Instruments, India. Before being sent as small rock slabs they were prepared using the rock saw at Adelaide University. Thins sections were requested to be polished standard 46 mm x 26 mm (30mm in thickness), with left over rock chips to be sent back to Adelaide upon completion. Thin sections were used for petrographic interpretation using an optical microscope at the University of Adelaide.

OBSERVATIONS

Field Observations/Petrology

There are two main lithologies identified in the BARTON and TALLARINGA areas. These include the unnamed granites and Lake Anthony gabbro and are found as discrete outcrops scattered across the western Gawler Craton intruding the Christie and Fowler Domains (Fig.1). Summary of sample locations and descriptions are listed in Table 1. The unnamed granites range from fine grained equigranulur to coarse grained K-feldspar megacrystic. The granites are all generally dominant in K-feldspar, quartz,

biotite and plagioclase. Plagioclase is difficult to identify in thin section due to extensive seritisation of some samples with little obvious twinning. Percentages used in petrological analysis are also referenced by hand specimen.

Lake Anthony outcrops are generally massive showing some foliation and comagmatic features. Mineralogically they are rich in hornblende, plagioclase and biotite and in almost all cases show seritisation of plagioclase. All samples show a lack of pyroxene in thin section suggests that the Lake Anthony gabbros may have been subject to metamorphic conditions where pyroxene has been thermally altered to amphibole, thus they could also be described as a metagabbro/amphibolite.

Wynbring Rock Hole (Samples 101 and 102)

A megacrystic granite (sample 102) sampled from Wynbring Rock Hole has been attributed to granites of the Tunkillia Suite (Teasedale, 1997). The granite outcrop can be described as massive with megacrysts of K-feldspar alignment defining a magmatic foliation, which is also seen in the melanosomes of biotite (Fig.5b). The granite is composed K-feldspar (50%), quartz (35%), biotite (10%), plagioclase (5%), zircon, titanite. Both quartz and biotite are intergrown between K-feldspar. K-feldspar can appear as perthite with quartz zoning. Quartz show recrystallization producing subgrains of >10 µm in size. The titanite crystals are very large in size up to 400 µm and are typically euhedral, characterized by tabular and diamond-like morphology. There is also chlorite alteration of biotite (Fig.6).

A porphyritic granite (sample 101) is located 16 Km east – south – east of Wynbring Rock Hole (Fig. 5a). The outcrop preserves a magmatic foliation trending north east – south west defined by melanosomes of biotite and mafic minerals. The granite is composed of quartz (40%), K-feldspar (40%), biotite (15%) plagioclase (<5%),

muscovite (<5%), zircon and titanite (up to 250 µm). K-feldspar generally occurs as microcline and biotite occurs as subhedral individual flakes. Titanite is found as brown, fully formed anhedral to euhedral crystals (Fig.6).

Edoldeh Rock Hole (samples 203, 204, 205, 306)

The appearance of comagmatism is found in a granite (sample 204), granodiorite (sample 203) and diorite (sample 205) suite 9.3 km west of Edoldeh Rockhole. Pegmatite veining crosscuts all units trending east – west occuring with epidote veining trending north – south with sharp contacts with the other units (Fig. 3). The granodiorite (sample 203) is dark grey medium grained and is composed of K-feldspar (35%), quartz (45%), biotite (15%), and plagioclase (5%). biotite is tabular up to 200µm. The equigranular granite is composed of K-feldspar (40%), quartz (40%), biotite (15%), and plagioclase (5%). Biotite is <100 µm. With quartz typically larger (>1000 µm). In outcrop the granodiorite and granite contain magmatic melanosomic foliations defined by biotite (Fig.5d). They also occur as xenocrystic enclaves within each other implying the comagmatic nature of the suite (Fig. 5c). A dark grey/black fine grained diorite occurs as globular enclaves solely within granodiorite (Fig. 5e).

An outcropping megacrystic granite (sample 306) is located 100 metres north of the aforementioned comagmatic suite. It occurs as small 2x2 m outcrop but is not seen in contact with the other units. The megacrystic granite is composed of K-feldspar (40%), quartz (40%), biotite (15%), plagioclase (5%). Biotite is (<100 µm) and is heavily sericite altered. All units at near Edoldeh Rock Hole are subject to abundant sericite alteration as well as epidote alteration.

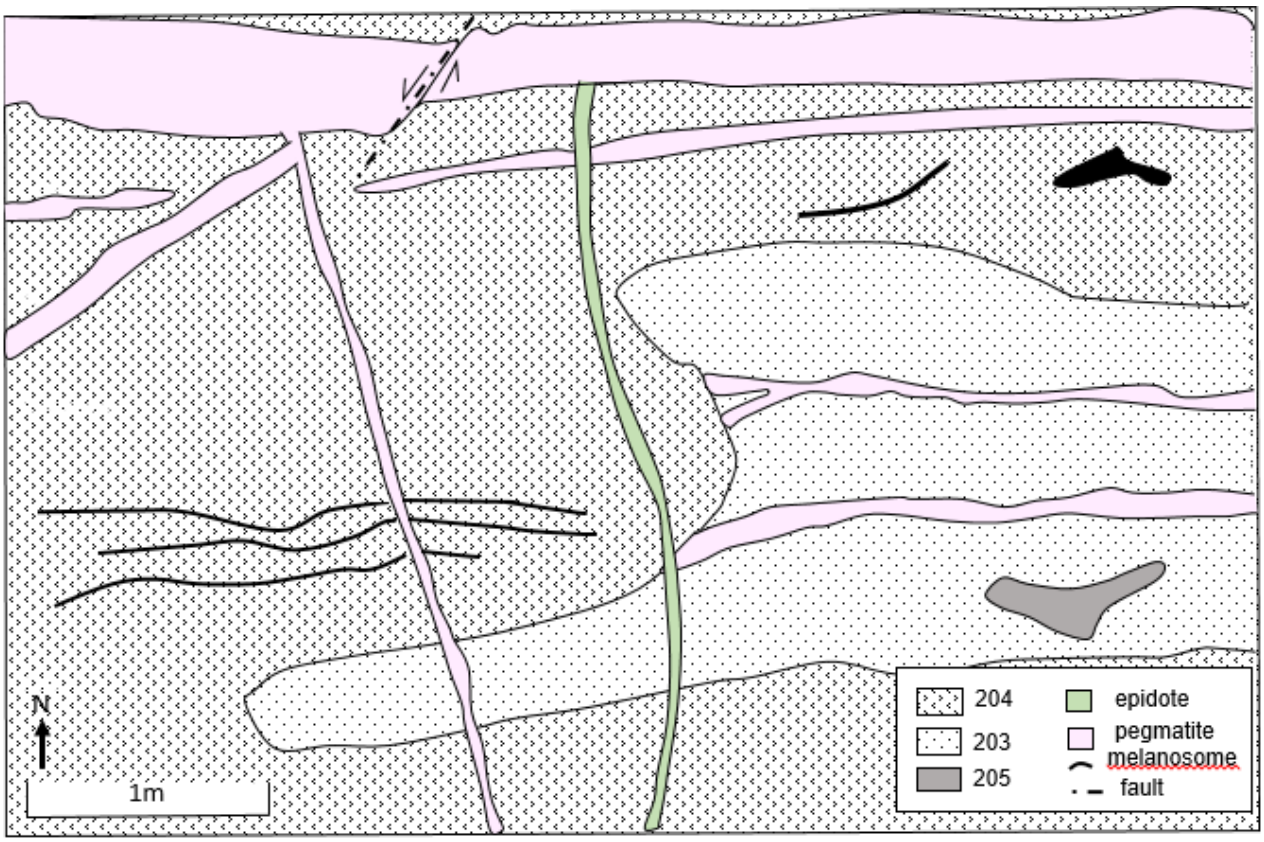

Figure 3: Field sketch overlay of unnamed granites from 9.3Km W of Edoldeh Rock Hole

Mobing Rock Hole (sample 307 and 308)

At Mobing Rock Hole a megacrystic granite (sample 307) is intruded by a finer grained granite (sample 308) mostly displaying sharp contacts, however some are gradational. The finer grain diorite preserves a foliation that trends north – east to south – west, which is parallel to the contact margin of the megacrystic granite. Similarly to Edoldeh Rock Hole there are K-feldspar rich pegmatite veins displaying an undulose margin crosscutting the megacrystic granite. The megacrystic granite is composed K-feldspar (45%), quartz (40%), biotite (15%) plagioclase (5%), zircon, titanite and apatite. Quartz commonly displays sub-grain domains and undulatory extinction as signs low-P deformation. Biotite is more dominate with tabular grain shape and seritisation is

present but less obvious than other granite samples. There are also large (>1000 μm) isotropic minerals present (Fig.6).

The very fine-grained granite has a composition of K-feldspar (40%), quartz (40%), biotite (20%) and zircon. In thin section quartz and biotite are very fine-grained (~10 μm) where biotite defines a foliation and contains phenocrysts of K-feldspar (up to 100 μm). Biotite occurs almost isotropically under CPL, but this may be due to the thin section being cut along the cleavage. Halos commonly occur around zircon and accessory crystals, and does not always follow the fabric defined by the biotite.

Lake Anthony (samples 509, 510, 511, 512, 513 and 514)

Two medium grained gabbros (511 and 512) occur as massive plutons which crop out on the northern edge of Lake Anthony. Outcrops appear to have a foliation that is parallel to the strike of the intrusion trending north – east. Figure (5f) shows one of the medium grained gabbros in outcrop. Both outcrop samples share mineralogical characteristics and are composed of plagioclase (40%) hornblende (25%), biotite (10%), and interstitial quartz 5%. Thin sections reveal hornblende occurs predominantly with biotite as clusters shows strong army green to lighter green pleochroism and is generally anhedral. (Fig.6). Sericite alteration is focussed on plagioclase throughout the samples.

A second location at Lake Anthony consists of a fine grained gabbro (sample 513), medium grained diorite (sample 514) and a granodiorite occuring in an apparent comagmatic suite (Fig.2). Fine grained gabbro enclaves are found within a medium grained diorite as well as within a granodiorite. The granodiorite is relatively K-feldspar rich and occurs as a zone between the fine grained gabbro and diorite, seemingly forming a felsic transitional boundary or chilled margin (Figs.4,5g). The fine-grained

gabbro comprises of plagioclase (40%), hornblende (30%), biotite (25%) and interstitial quartz (<5%). Also contains a high abundance of finer isotropic minerals.

The composition of the diorite consists of plagioclase (40%), hornblende (25%), quartz (20%) biotite (15%). Where biotite occurs almost exclusively with hornblende and hornblende exhibits strong green pleochroism. Quartz is more prominent becoming phenocrystic compared to the other samples and there is a relatively smaller percentage of isotropic minerals.

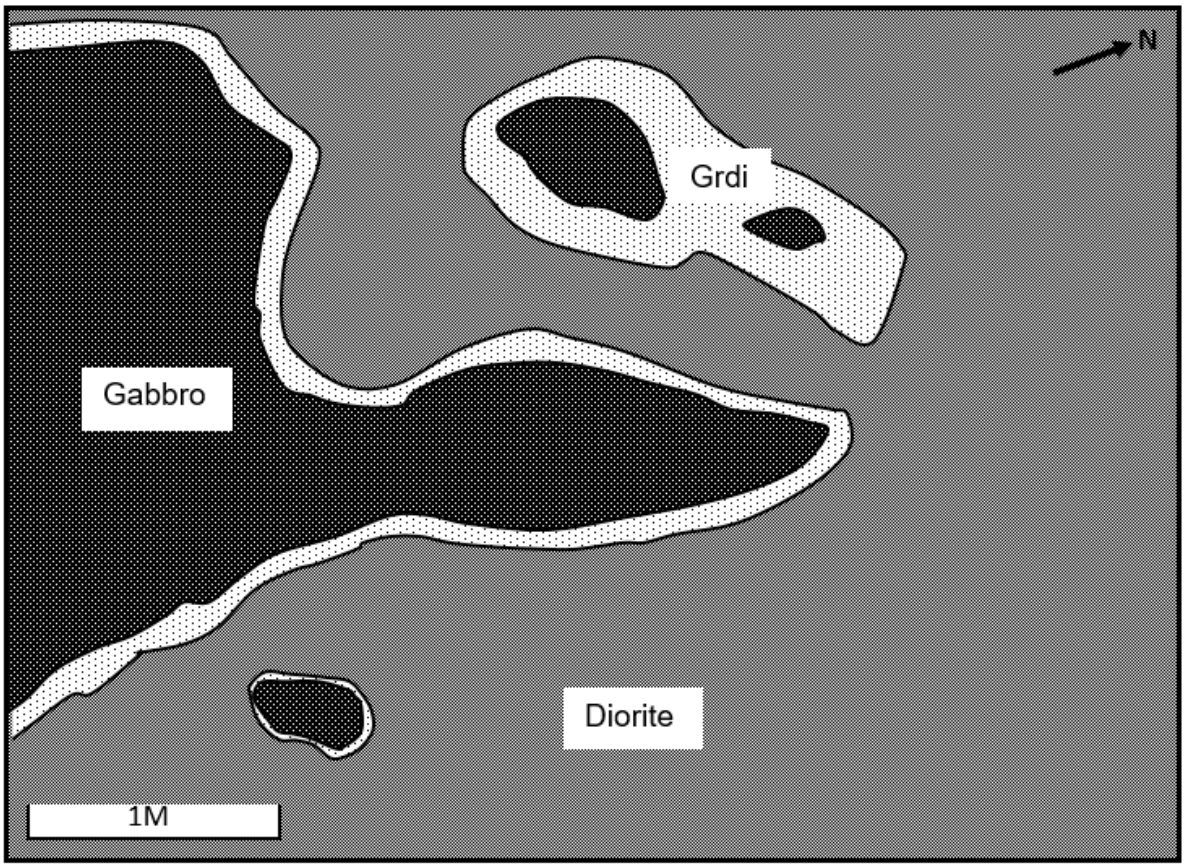

Figure 4: Field sketch overlay of Lake Anthony location showing relationship between the gabbro (sample 513), diorite (sample 514) and granodiorite (Grdi) (white zone separating the two other two units). Sketch shows a larger view from the field photo in Figure 5g.

Table 1: Summary of samples, including location, rock type, unit, descriptions and type of analysis.

SAMPLE	LOCATION	EASTING	NORTHING	ZONE	ROCK - TYPE	UNIT	DESCRIPTION	GEO-CHRON	GEO-CHEM	THIN - SECTION	Sm-Nd
101	16 km ESE Wynbring	375488	6615526	53	Granite	Tunkillia	Porphyritic, medium grained, plg-qtz-bi-kfld with fabric		✓	✓	
102	Wynbring Rocks	360060	6619090	53	Granite	Tunkillia	Megacrystic (Kfld), coarse grained, plg-qtz-bi-kfld		✓	✓	
203	9.3 km W of Edoldeh Rockhole,	339041	6629260	53	Granodiorite	Tunkillia	Dark grey, medium grained bi-kfld-qtz with epidote alteration		✓	✓	
204	9.3 km W of Edoldeh Rockhole,	339041	6629260	53	Granite	Tunkillia	Light grey, equigranular, medium grained bi-qtz-plag-kfld		✓	✓	
205	9.3 km W of Edoldeh Rockhole,	339041	6629260	53	Diorite	Tunkillia	Dark grey/black, fine grained				
306	9.3 km W of Edoldeh Rockhole,	339032	6629349	53	Granite	Tunkillia	Megacrystic (Kfld), coarse grained	✓	✓	✓	✓
307	Mobella Soak/Mobing Rockhole	315877	6662310	53	Granite	Tunkillia	Megacrystic, coarse grained bi-qtz-kfld subvertical gneissic foliation	✓	✓	✓	✓
308	Mobella Soak/Mobing Rockhole	315877	6662310	53	Granite	Tunkillia	Fine grained bi-qtz granite dykes and sills with foliation		✓	✓	
509	Lake Anthony	338686	6687486	53	Granodiorite	Peter Pan Super Suite	Equigranular (1-2mm) lag samples - NOT INSITU				
510	Lake Anthony	338686	6687486	53	Granite	Peter Pan Super Suite	Equigranular (1-2mm) lag samples - NOT INSITU			✓	
511	Lake Anthony	338697	6687412	53	Gabbro	Peter Pan Super Suite	Dark grey, massive, medium grained qtz-hbl-plg-bi		✓	✓	✓
512	Lake Anthony	337298	6687020	53	Gabbro	Peter Pan Super Suite	Dark grey, massive, medium grained qtz-hbl-plg-bi		✓	✓	
513	Lake Anthony	337394	6687677	53	Gabbro	Peter Pan Super Suite	Dark grey, fine-medium grained qtz-hbl-plg-bi		✓	✓	✓
514	Lake Anthony	337394	6687677	53	Diorite	Peter Pan Super Suite	Medium-coarse grained qtz-hbl-bi-plg with qtz phenocrysts and granite zoning	✓	✓	✓	✓

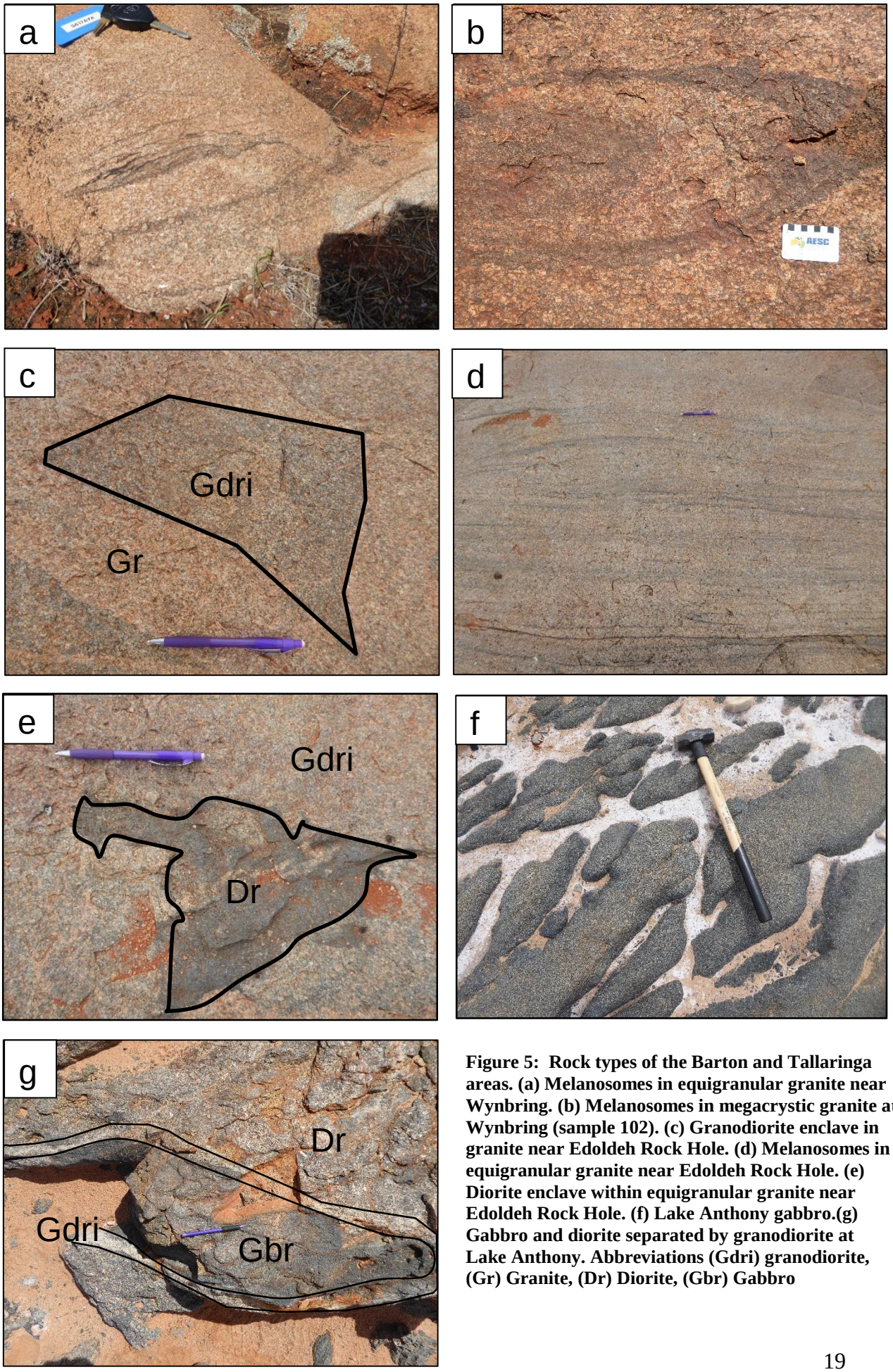

Figure 5: Rock types of the Barton and Tallaringa areas. (a) Melanosomes in equigranular granite near Wynbring. (b) Melanosomes in megacrystic granite at Wynbring (sample 102). (c) Granodiorite enclave in granite near Edoldeh Rock Hole. (d) Melanosomes in equigranular granite near Edoldeh Rock Hole. (e) Diorite enclave within equigranular granite near Edoldeh Rock Hole. (f) Lake Anthony gabbro.(g) Gabbro and diorite separated by granodiorite at Lake Anthony. Abbreviations (Gdri) granodiorite, (Gr) Granite, (Dr) Diorite, (Gbr) Gabbro

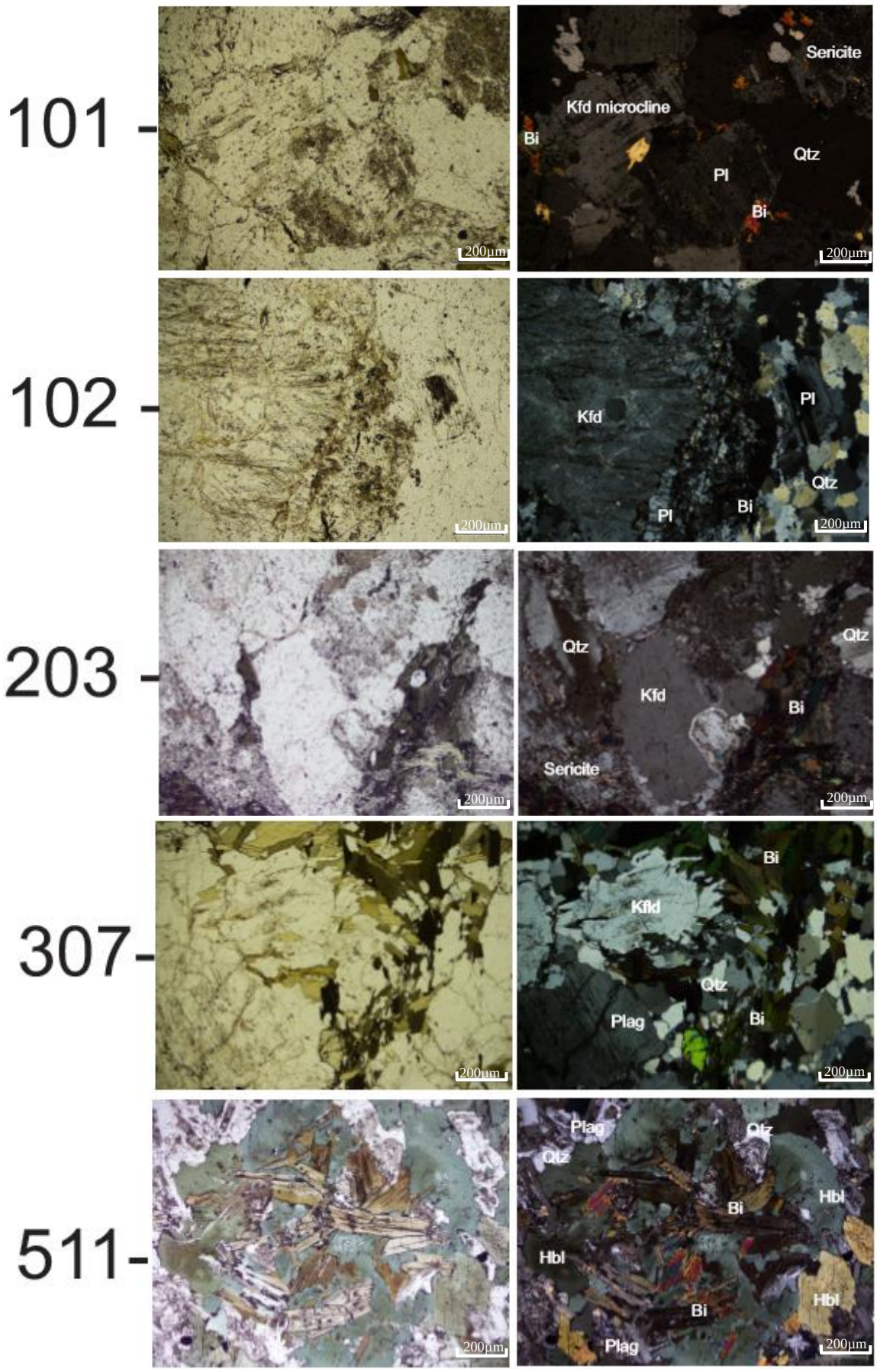

Figure 6: Thin section images with sample names adjacent. Mineral abbreviations (Kfd) Potassium feldspar, (Bi) Biotite, (Qtz) Quartz, (Pl) Plagioclase feldspar.

U-Pb Zircon Geochronology

A summary of geochronology results are reported in Table 2, and complete geochronological data is in Appendix.A. Three samples were initially chosen for U – Pb zircon geochronology. U – Pb monazite geochronology was attempted on sample 306, however ^{204}Pb (common lead) contamination was apparent, hindering accurate results. U – Pb monazite data is not discussed here but can be found in Appendix. A. U – Pb zircon geochronology was collected for a granite from Mobing Rock Hole (sample 307) and a diorite from Lake Anthony (sample 514). Zircons which had a discordancy of >10% for the granite were discarded and not included in age calculations. For the diorite a cut off discordancy of >5% was used as there was > 200 analyses obtained. Weighted average ages calculated for each sample using ^{207}Pb/^{206}Pb can be (Fig.8c,f). Based on probability density plots populations of zircons were found likely to be inherited are shown in Figure 8b,e. Cathodoluminescence (CL) images with position of analysed spots as well as age measured are shown (Fig.7)

Table 2: Geochronology data for the unnamed granites and Lake Anthony gabbro samples

Sample No.	Lithology	Spots Analysed	Spots Used	Zircon Ages	MSWD	Concordance
307	Granite	127	109	1694.5±6.4	2.4	<10%
514	Diorite	231	154	1712±6	5.4	<5%

Sample 307, Granite from Mobella Soak/Mobing Rock Hole

Zircon grains are yellow/brown in colour and have prismatic and euhedral shape. They measure 150-320µm in size. Grains exhibit well developed growth zoning typical of crustal granites. Some grains also show local recrystallisation indicative of late magmatic processes. Representative grains are shown in Figure 7a, b, c. Of 127 cores

analysed 109 were used in age calculation using <10% concordance. Crystallisation age using a $^{207}Pb/^{206}Pb$ weighted average is calculated to be 1694.5±6.3 (MSWD = 2.3; Fig.8c). A grouping and separate peak of 5 analyses revealed by the probability density plot (Fig.8b) gives a possible inheritance age of ~1809. Concordant analyses are shown on Figure 8(a).

Sample 514, Diorite, Lake Anthony

The zircons of sample 514 are colourless or brown/yellow, prismatic and measure from 100 to >350µm in size and show sharp prismatic terminations. Grains display various internal textures, though predominantly they display broad to thin oscillatory zonation and in many cases, no to weak internal zonation (Fig.7 d,e,f). Of 231 spots analysed 154 were used in age calculation using <5% concordance. Crystallisation age using a $^{207}Pb/^{206}Pb$ weighted average is calculated to be 1712.4±6.0 (MSWD = 5.4; Fig. 6f). A grouping and separate peak of 11 analyses revealed by the probability density plot (Fig.7e) gives a probable inheritance age of ~1810 Ma. Analyses showed general spread along the concordant curve rather than a population grouped together (Fig. 6d)

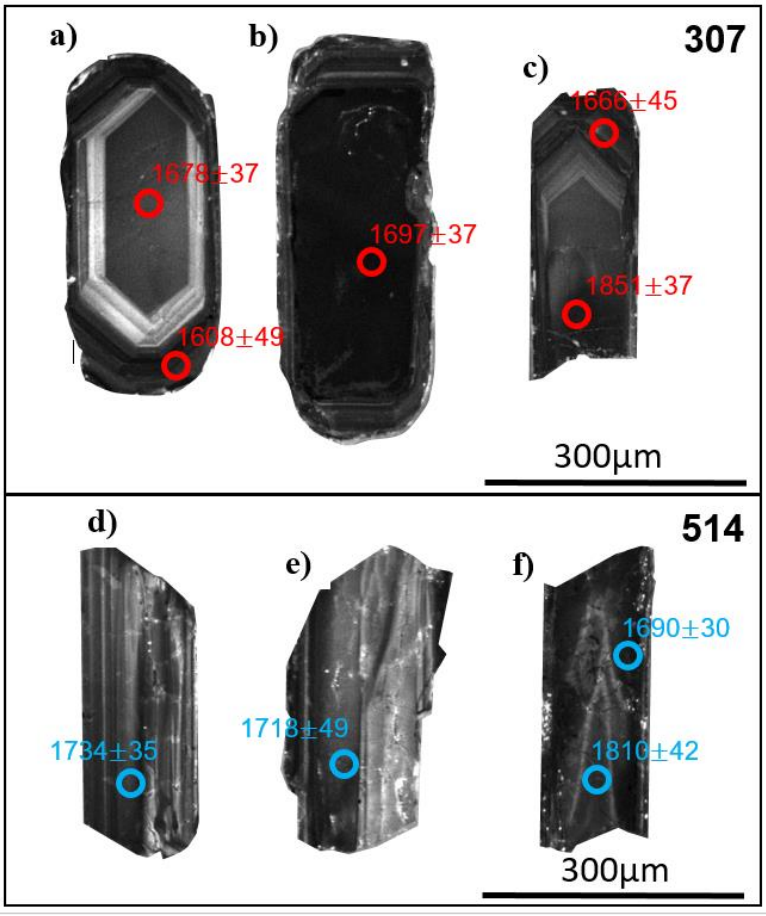

Figure 7: Cathodoluminscence images of zircons 307 and 514. Targeted analyses are shown in red (sample 307) and blue (sample 514). Probable inherited cores are seen in (c) and (f) for both samples. Ages calculated for each analyses are also shown.

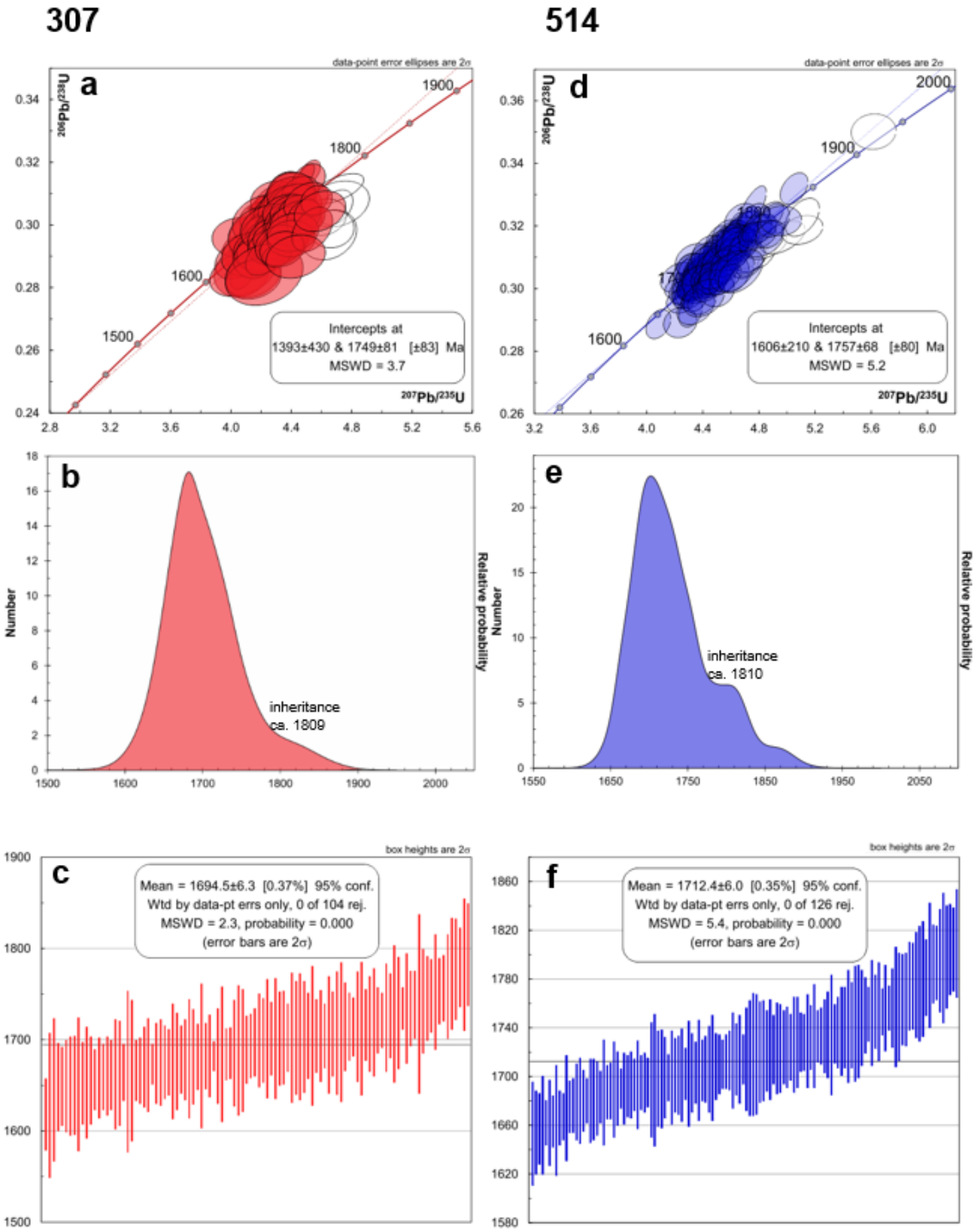

Figure 8: (a), (d) Concordia plots. Spot analyses are shown in red (307) and blue (514) and analyses thought to be inherited shown in white. (b), (e) Probability density plots showing age peaks and probable inheritance. (c), (f) Weighted mean average distributions for each sample.

Geochemistry

MAJOR ELEMENTS

Major geochemical results for all samples are reported on Table 3, trace and geochemical datasets are reported on Table 4.

The unnamed granites plot as ferroan on Fe8-SiO2 and on the MALI (modified alkali lime index) diagram. They fall predominantly within the calc-alkalic fields and High-K calk-alkaline to shoshonite fields on K_2O vs SiO_2 tectonic classification diagrams by Frost et al. (2001) and Peccerillo and Taylor (1979) respectively. Using Nb v Y (Pearce et al. 1984) the granites show an affinity towards volcanic arc and collisional tectonic regimes and show some spread to within plate settings. The Lake Anthony gabbros plot as enriched tholeiitic on the AFM diagram (Fig.11)

On the R1-R2 diagrams (Fig.9) (De la Roche, 1989) the samples plot into distinctive compositional fields of granites/granodiorite and gabbros/diorite. The unnamed granites are weakly peraluminous and rich in K-feldspar. Harker variation diagrams for both suites are displayed in Figure 13, the unnamed granite samples have a SiO_2 range of 69.3wt% - 74.2wt% and the Lake Anthony samples have a SiO2 range of 52.3-65.5wt%. The unnamed granites display inverse correlations between Al_2O_3, CaO, FeOt, MgO and TiO_2 with increasing SiO_2 forming fractional crystallisation trends controlled by K-feldspar. Samples P_2O_5, NaO, K_2O abundances are variable when plotted against SiO_2. All samples display similar major element abundances except for the megacrystic granite (sample 307) which is relatively enriched in TiO_2, $P2O_5$ and FeOt.

The Lake Anthony gabbro display decreasing abundances of Al_2O_3, TiO_2, FeOt and P2O5 against increasing SiO_2. Na_2O, CaO and MgO do not define trends and appear scattered with respect to SiO_2. K_2O and SiO_2 display a positive correlation.

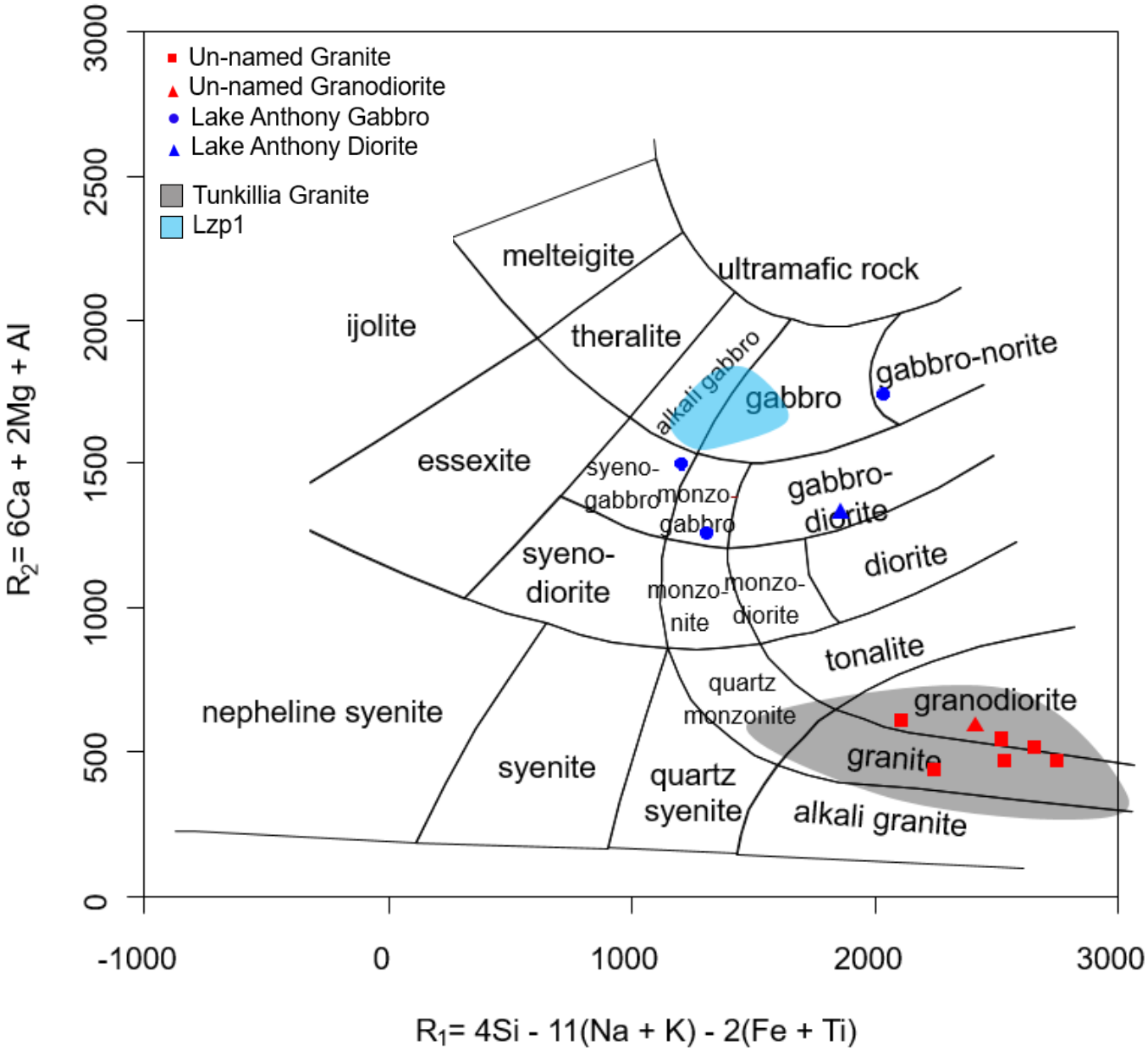

Figure 9: Plutonic rock classification after De la Roche et al. (1980) for unnamed granite (red) and Lake Anthony (blue) Also shown are fields of the Tunkillia suite (grey, Payne et al., 2010) and mafic rocks of the Peter Pan SuperSuite (Blue; inpubGSSAdata)

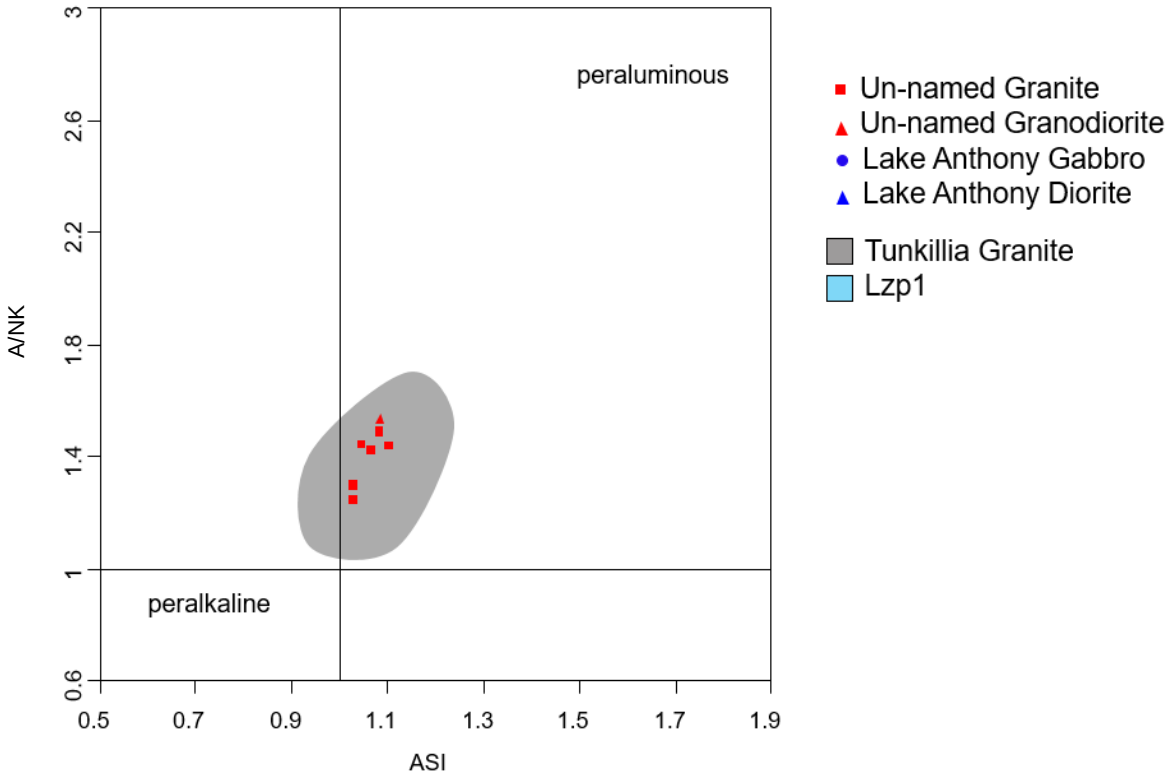

Figure 10: ASI plot after Shand (1943) showing unnamed granites and Lake Anthony samples against Tunkillia suite (grey field, Payne et al., 2010)

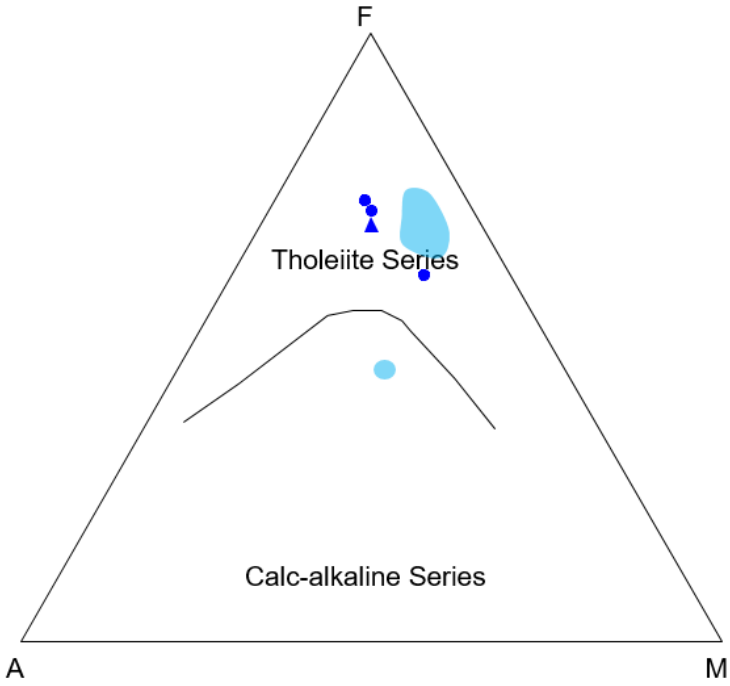

Figure 11: AFM classification diagram after Irvine and Bargar (1971) Lake Anthony plotted against mafic rocks of the Peter Pan SuperSuite (Blue field; unpubGSSAdata)

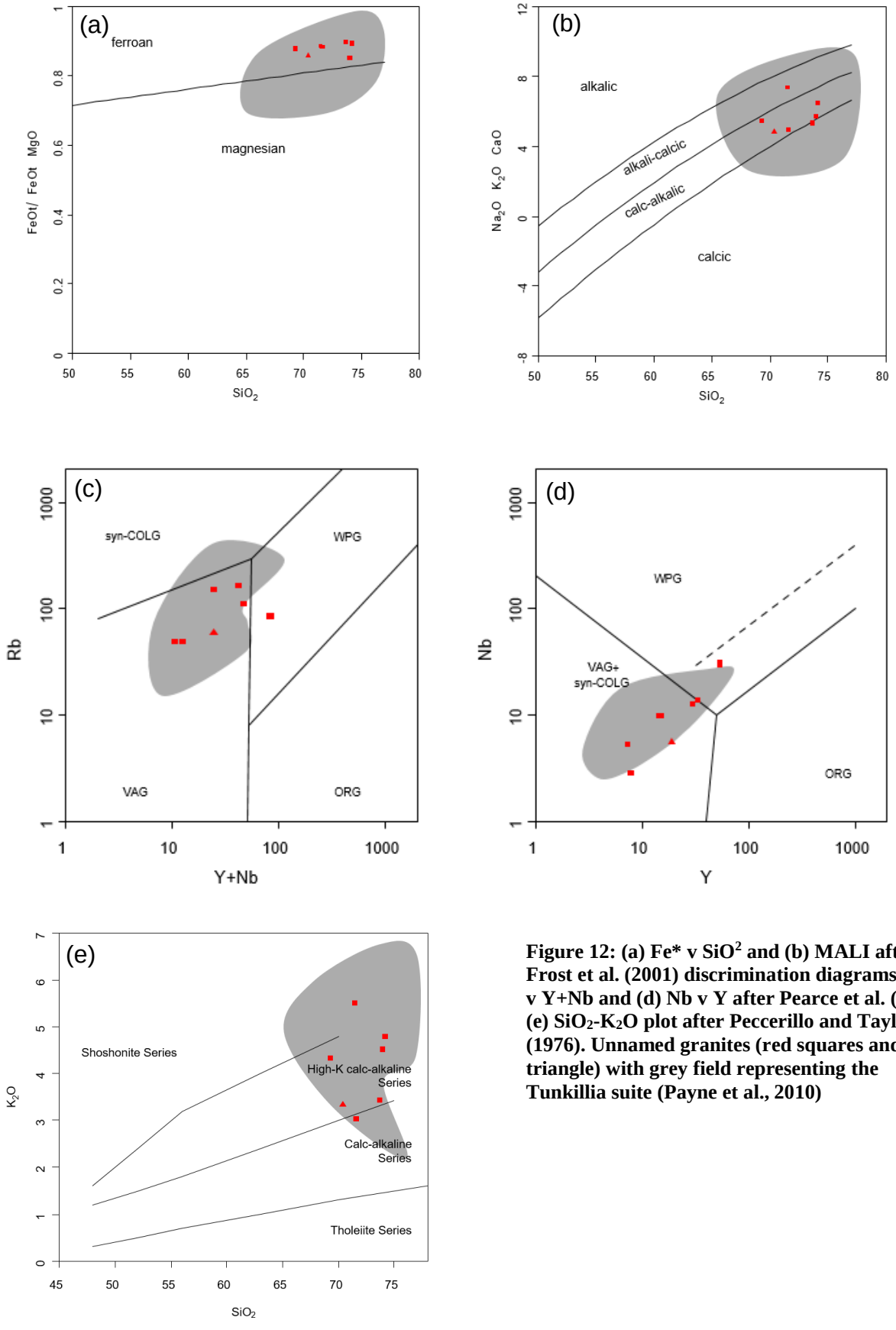

Figure 12: (a) Fe* v SiO^2 and (b) MALI after Frost et al. (2001) discrimination diagrams (c) Rb v Y+Nb and (d) Nb v Y after Pearce et al. (1984) (e) SiO_2-K_2O plot after Peccerillo and Taylor (1976). Unnamed granites (red squares and triangle) with grey field representing the Tunkillia suite (Payne et al., 2010)

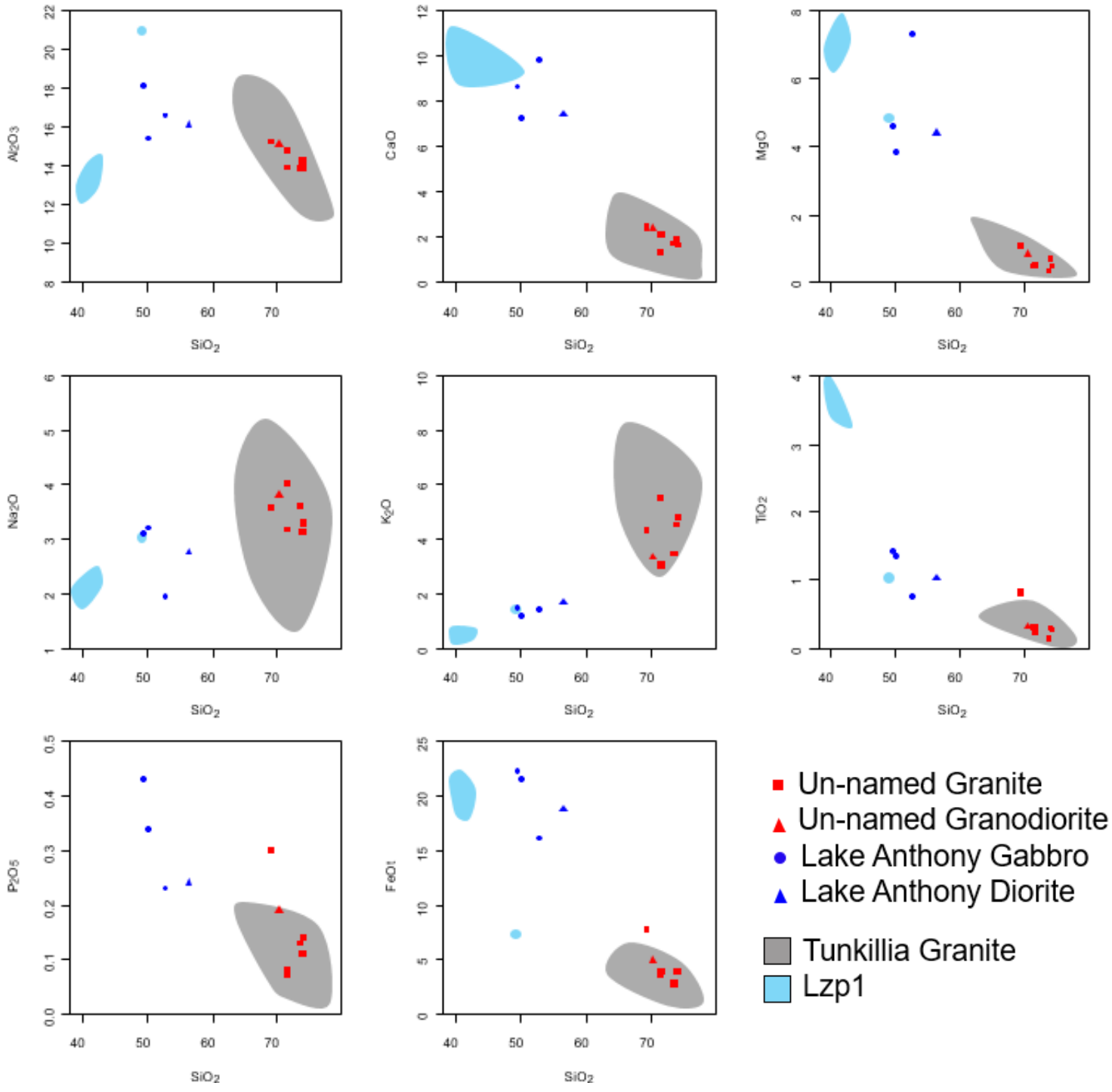

Figure 13: Harker diagrams of Major elements vs SiO_2. Fields and points as per legend. Tunkillia suite (grey field; Payne et al., 2010 and mafic Peter Pan SupersSuite Lzp1 (blue field; unpubGSSAdata)

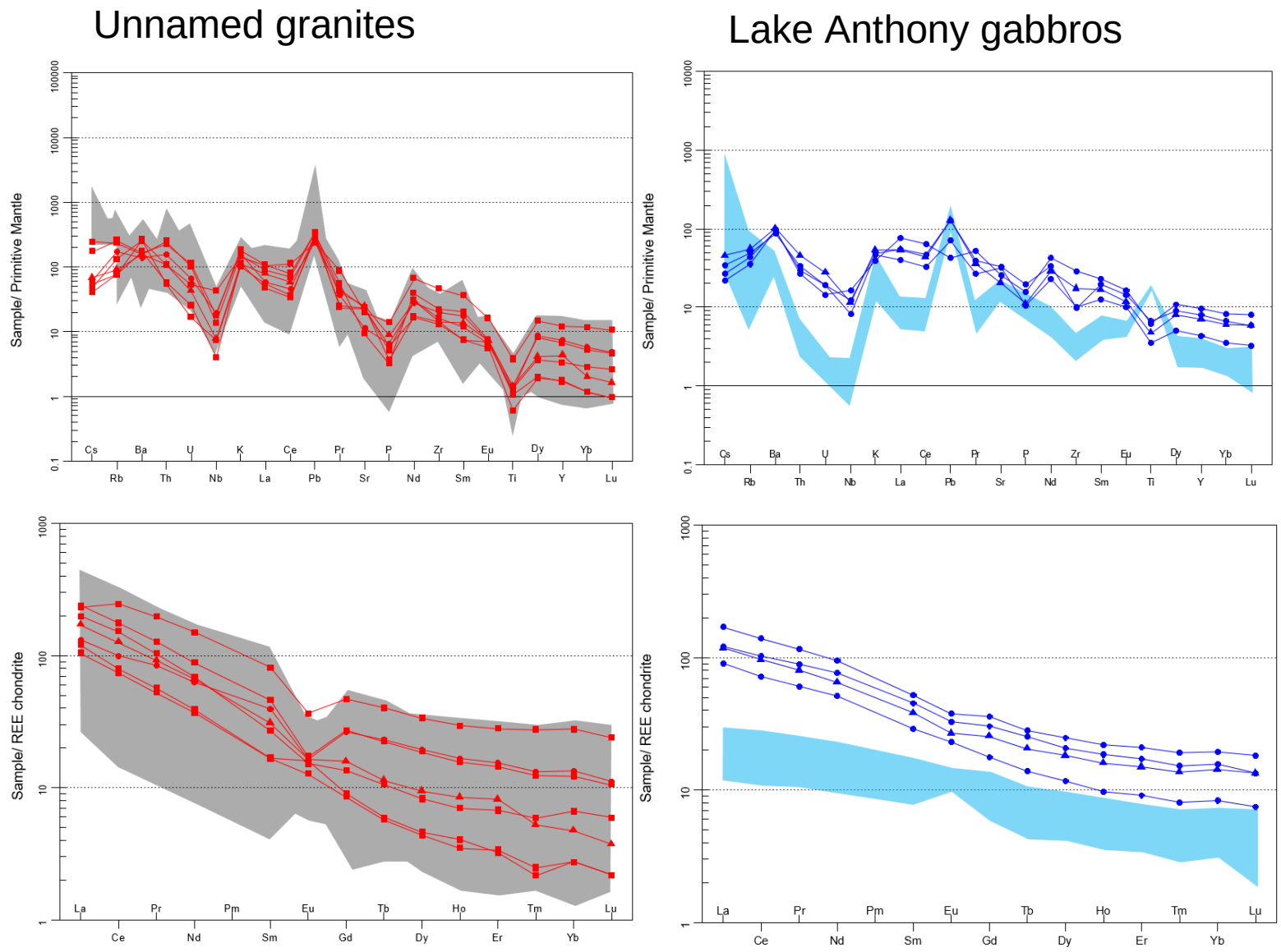

Figure 14: REE chondrite normalised (Boynton, 1984) and Primitive mantle normalised spider plots (Sun & McDonough, 1989) for unnamed granite and Lake Anthony gabbros. Blue fields represent Lzp1 Gabbro (unpubGSSA) and grey fields represents the Tunkillia suite (Payne et al., 2010)

TRACE ELEMENT AND RARE EARTH ELEMENTS

Trace element geochemical results can be seen in Table 4. Trace element and rare earth element (REE) spider plots normalised to primitive mantle and chondrite following Sun and McDonough (1989), and Boynton (1984) respectively, are presented in Figure 14. Primitive mantle normalised trace element diagrams for the unnamed granites display similar patterns for all samples with variable depletions of Nb, P and Ti. Chondrite

normalised REE plots show relatively flat to concave Heavy rare earth element (HREE) patterns for the unnamed granites (Fig. 14). Eu/Eu* anomalies are predominately negative (~0.4-1.4) with two out of the eight granitic samples having positive anomalies. Ratio between LREE and HREE enrichment is substantial with La_n/Yb_n values of 9.7-44.

Primitive mantle normalised trace element diagrams for Lake Anthony gabbro display little variance between samples and notable depletions in Nb, P and Ti. Chondrite normalised REE plots display high LREE patterns which are relatively enriched compared to HREE with La_n/Yb_n ratios of 7.8-10.8. The majority of Eu/Eu* anomalies are marginally negative with values of (~-0.8). Lake Anthony samples are generally more enriched in both HSFE and LREE (Fig.14)

Table 3: Major element data for the unnamed granites and Lake Anthony gabbros

Sample	101	102	203	204	306	307	308	511	512	513	514
Lithology	Granite	Granite	Grano-diorite	Granite	Granite	Granite	Granite	Gabbro	Gabbro	Gabbro	Diorite
SiO_2	74.0	71.5	70.4	73.7	71.6	69.3	74.2	52.8	49.6	50.2	56.5
$Al2O_3$	14.3	13.9	15.1	13.9	14.8	15.2	13.8	16.6	18.1	15.4	16.1
FeO	1.9	1.8	2.4	1.4	1.9	3.8	1.9	8.1	11.2	10.8	9.4
Fe_2O_3	2.1	2.0	2.7	1.5	2.1	4.3	2.1	9.0	12.4	12.0	10.4
CaO	1.9	1.3	2.3	1.7	2.1	2.4	1.6	9.9	8.6	7.2	7.4
MgO	0.7	0.5	0.8	0.3	0.5	1.1	0.5	7.3	4.6	3.8	4.4
K2O	4.5	5.5	3.3	3.4	3.0	4.3	4.8	1.4	1.5	1.2	1.6
Cr_2O_3	<0.01	<0.01	<0.01	<0.01	<0.01	<0.01	<0.01	0.0	<0.01	<0.01	<0.01
TiO_2	0.3	0.3	0.3	0.1	0.2	0.8	0.3	0.8	1.4	1.3	1.0
MnO	0.0	0.0	0.0	0.0	0.0	0.1	0.0	0.2	0.2	0.2	0.2
P_2O_5	0.1	0.1	0.2	0.1	0.1	0.3	0.1	0.2	0.4	0.3	0.2
SrO	0.1	0.0	0.1	0.1	0.1	0.0	0.0	0.1	0.1	0.1	0.0
BaO	0.1	0.1	0.1	0.1	0.2	0.2	0.1	0.1	0.1	0.1	0.1
Total	101.7	98.7	99.9	99.1	99.3	101.9	101.1	101.6	101.0	95.8	101.7
LOI	0.5	0.3	0.8	0.5	0.6	0.4	0.3	1.5	1.0	0.8	1.0

Table 4: REE and trace element data for unnamed granite and Lake Anthony gabbros

Sample	101	102	203	204	306	307	308	511	512	513	514
Lithology	Granite	Granite	Grano-diorite	Granite	Granite	Granite	Granite	Gabbro	Gabbro	Gabbro	Diorite
Trace element (ppm)											
Ag	<0.5	<0.5	<0.5	<0.5	<0.5	<0.5	<0.5	<0.5	<0.5	<0.5	<0.5
As	<5	<5	<5	<5	<5	<5	<5	<5	<5	<5	<5
Cd	<0.5	<0.5	<0.5	<0.5	<0.5	<0.5	<0.5	<0.5	<0.5	<0.5	<0.5
Co	25	24	23	26	56	24	23	37	38	43	44
Cu	10	1	<1	1	<1	1	<1	29	7	4	12
Zn	32	34	56	27	42	74	37	78	119	129	95
Ba	1080	1160	1075	1205	1860	1760	971	615	662	670	705
Cr	10	10	10	10	10	10	10	90	10	10	40
Cs	1.93	1.37	0.54	0.32	0.43	0.37	0.47	0.27	0.21	0.17	0.36
Ga	17.6	18.2	20.8	16.7	18.8	21.9	15.3	18.6	22.7	24.5	21
Hf	4.9	6.4	4.3	3.8	4.1	11.5	5.9	2.8	2.9	7.5	4.7
Li	10	20	10	<10	10	10	<10	10	10	10	10
Mo	<1	1	1	<1	<1	2	<1	1	<1	<1	1
Nb	9.6	12.7	5.5	2.8	5.2	30	13.8	5.9	8.8	11.8	8.2
Ni	4	1	4	<1	1	1	1	52	3	9	15
Pb	23	24	17	22	19	17	21	5	9	3	9
Rb	149	162.5	57.7	48.4	49.2	84.5	108.5	31.3	27.8	22.3	35
Sc	3	3	4	2	3	11	3	28	26	28	22
Sn	2	1	1	<1	1	3	2	1	1	1	1
Sr	488	195	517	469	489	416	242	673	699	534	428
Ta	0.9	1	0.3	0.3	0.3	2.1	1.4	0.3	0.5	0.5	0.4
Th	21	19.2	9.07	4.9	4.61	9.17	13.2	2.83	2.5	2.24	3.88
Tl	<10	<10	<10	<10	<10	<10	<10	<10	<10	<10	<10
U	2.1	2.35	0.88	0.53	0.35	1.1	1.37	0.4	0.4	0.3	0.58
V	34	30	45	30	30	59	24	190	278	312	246
W	195	194	154	211	460	145	191	80	83	101	116
Y	15	30.2	19.5	7.9	7.6	54.4	33.8	19.7	36.8	43.2	31.9
Zr	181	247	160	144	157	514	222	112	109	322	194
REE (ppm)											
Ce	122.5	142	102	59.6	64.2	199	79.9	58	83.1	113	77.7
Dy	2.64	6.02	3.04	1.4	1.47	10.8	6.28	3.75	6.61	8	5.85
Er	1.41	3.03	1.71	0.71	0.67	5.86	3.23	1.92	3.62	4.39	3.14
Eu	1.11	1.27	1.21	0.93	1.17	2.68	1.2	1.69	2.42	2.78	1.96
Gd	3.49	7.05	4.11	2.2	2.33	12.05	6.81	4.58	7.87	9.34	6.58
Ho	0.5	1.12	0.61	0.25	0.29	2.1	1.2	0.7	1.34	1.59	1.15
La	61.3	73.9	53.2	32.3	37.2	72	40.5	28	37.7	52.7	36.7
Lu	0.19	0.34	0.12	0.07	0.07	0.77	0.36	0.24	0.43	0.59	0.43
Nd	41.1	53.1	39.7	22.3	23.5	90.1	37.5	30.6	45.7	56.9	39
Pr	12.55	15.5	11.2	6.4	6.91	24	10.2	7.44	10.95	14.25	9.78
Sm	5.26	8.95	6.04	3.27	3.25	15.85	7.67	5.7	8.79	10.15	7.44
Tb	0.5	1.06	0.54	0.27	0.28	1.9	1.09	0.66	1.19	1.33	0.97
Tm	0.19	0.4	0.17	0.08	0.07	0.89	0.43	0.26	0.49	0.62	0.44
Yb	1.38	2.56	0.99	0.57	0.57	5.75	2.81	1.75	3.27	4.08	2.98
Ratios											
Eu/Eu*	0.79	0.49	0.74	1.06	1.3	0.59	0.51	1.01	0.89	0.87	0.86
Lan/Ybn	30.02	19.51	36.31	38.29	44.1	8.46	9.74	10.81	7.79	8.73	8.32
Lan/Smn	7.53	5.34	5.69	6.38	7.4	2.94	3.41	3.17	2.77	3.36	3.19

Eu/Eu*: a measure of the Eu anomaly relative to the concentrations of Sm and Gd on a REE plot.
Lan/Ybn (La/0.367)/(Yb/0.248) (normalising value from Taylor & Mclennan, 1985)
Lan/Smn(La/0.687)/(Sm/0.444)(normalising value from Sun and Mcdonough, 1989)

SAMARIUM – NEODYNIUM

Sm – Nd results for the unnamed granites and Lake Anthony gabbro are presented in Table.5 and growth evolution diagram displayed in Figure 15. The depleted mantle and CHUR evolution lines are indicated as well as data sets of the eastern and western Tunkillia Suite (Payne et al., 2010) and Lzp1 gabbro (GSSA). Also shown are the general evolution trends for the Archean Mulgathing crust (GSSA). εNd values for the unnamed granite samples are shown to be relatively evolved where $\varepsilon Nd_{(1695\ Ma)}$ = -5.3 and -7.2 falling within the Archean crustal domain. Values for the Lake Anthony gabbro are also relatively negative with the samples plotting $\varepsilon Nd_{(1712\ Ma)}$ = -3.3 and -4.9.

Table 5: Radiogenic Isotopic data for selected samples of the unnamed granite and Lake Anthony gabbros.

Sample	Lithology	Sm(ppm)	Nd(ppm)	$^{147}Sm/^{144}Nd$	$^{143}Nd/^{144}Nd$	Error	εNd(0)	εNd(T)	TDM (Ma)
306	Granite	3.1	21.3	0.0893	0.511073	0.000002	-30.5	-7.23	2516
307	Granite	15.9	89.2	0.1078	0.511379	0.000002	-24.6	-5.27	2517
511	Gabbro	6.0	33.0	0.1111	0.511497	0.000001	-22.3	-3.49	2425
513	Gabbro	9.8	52.6	0.1124	0.511439	0.000002	-23.4	-4.92	2425
514	Diorite	7.2	38.2	0.1134	0.511446	0.000002	-23.6	-4.99	2425

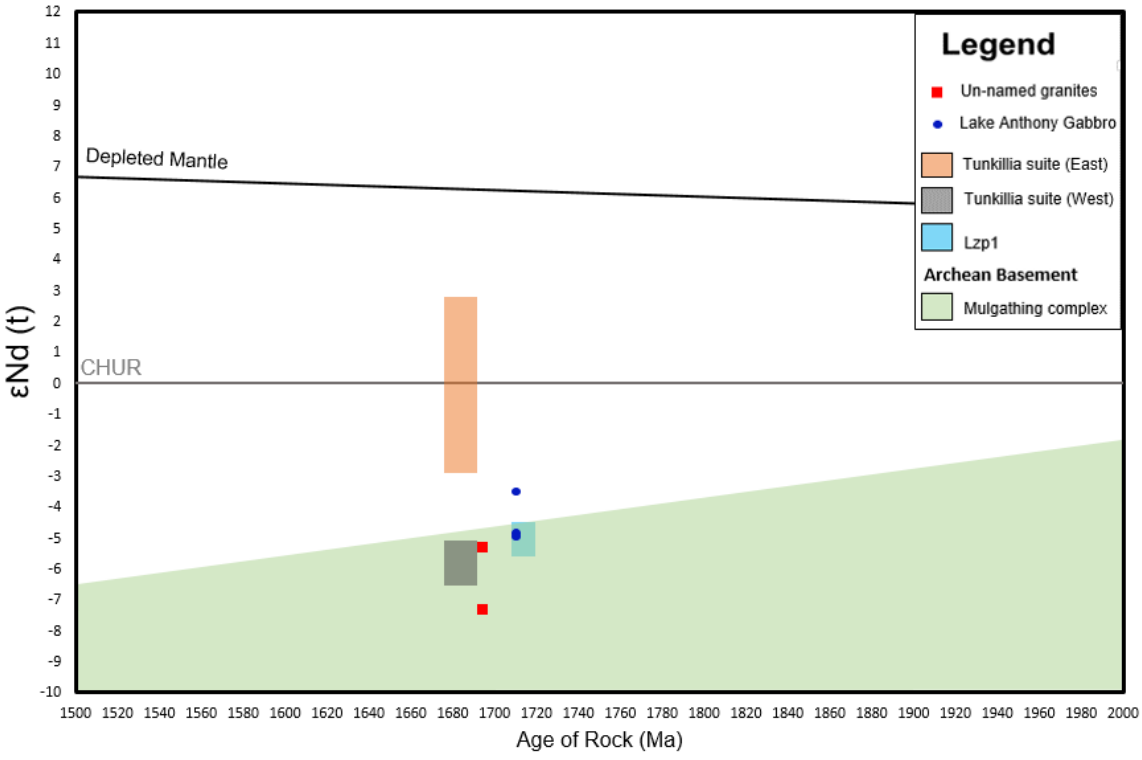

Figure 15: Sm – Nd evolution diagram for unnamed granites and Lake Anthony gabbro. Also displayed are the Tunkillia suite (Payne et al. 2010) and Lzp1 (unpubGSSA) and field for the local crustal basement the Mulgathing Complex (unpubGSSA)

DISCUSSION

Field Relationships and Emplacement Timing

Both the unnamed granites and Lake Anthony gabbros individually exhibit evidence for comagmatism and magma mixing features, as well as exhibiting age relative emplacement relationships between lithologies. Traditionally variation within suites can be the attributed to several processes such as magma mixing or mingling, assimilation, fractional crystallization, varying degrees of separation of restite from a melt, or a combination of those processes (Chapell, 1996). In all cases the outcrops were non-deformed, only showing magmatic foliation with no deformation fabrics observed. With this consideration the following is a summary of some of these relationships observed at location.

WYNBRING

Evidence of possible magma mingling can be seen in the megacrystic granite from Wynbring rocks. The megacrystic granite exhibits reverse zoning in some grains of the megacrysts where rounded K-feldspar crystals have been mantled by plagioclase, similar to Rapakivi granite textures (Dempster et al., 1993). This is suggestive of a crustal derived magma possibly coming into contact with a more mafic melt. However, there are no mafic enclaves to provide further evidence of this.

EDOLDEH ROCK HOLE

The unnamed granite and granodiorite from east south east of Edoldeh Rock Hole occur as enclaves within one another. This suggests that both units must have been magmatic or at least partially molten at the same time, thus qualifying the suite as comagmatic.

Mineralogical similarities and major element trends seen in variation diagrams favour fractional crystallization of melt (Fig.12). The diorite is perhaps further evidence of fractionation, or it may well be the result of magma mingling. Many workers conclude that mafic enclaves represent either cognate material or globules of basaltic magma quenched in a granitic host (Chappell, 1996). However, due to a lack of geochemical and petrological data of that unit, magma mingling cannot be substantiated (Fig.4c). Minor mafic enclaves such as these are also noticed somewhat uncommonly in other Tunkillia suite outcrops (Payne et al., 2010). Observations suggest that the diorite was the first to crystallise, being solely found as an enclave within the granodiorite. The granodiorite crystallising second was likely still partially magmatic when the granite intruded, evidenced by relatively sharp contacts in some enclaves of the granodiorite within the granite (Fig. 5e). Late stage pegmatite veining followed, likely as the last hydrous phase of differentiation processes or possibly from hydrothermal processes associated with later events.

MOBING ROCK HOLE

Mobing Rock Hole consists of a very fine-grained granite dyke intruding a K-feldspar megacrystic granite. The very fine-grained granite displays a crystal size of biotite and quartz of less than 10 µm. As the texture of igneous rocks are in large part functions of both cooling rate and melt composition (Fenn, 1977), the fine grained granite shows evidence for a very rapid crystallisation, which is likely to be under near surface conditions relative to the megacrystic granite. The fine grained granite is the most SiO_2 rich out of any of the unnamed granite samples and this suggests it's an end member for fractional crystallisation process.

LAKE ANTHONY

Apparent comagmatism is seen in the Lake Anthony rocks between the fine-grained gabbro and diorite units. The two units are found to be separated by a third more felsic granite to granodiorite. This is inferred to be a transitional area where a reaction between the intruding gabbro and the diorite has taken place. The gabbro was likely at a high temperature relative to the diorite, slowing down cooling and producing a chilled contact precipitating the more felsic minerals (Fig.4). Unfortunately age relationships cannot be corroborated with geochronological data, however given the gabbro occurs as enclaves within the diorite, it is likely that the diorite has intruded the older gabbroic body. Parallel REE patterns of the two units (Fig.12) and an almost identical Nd isotopic nature (Table 5) suggest that they were derived from the same source and differences may be the result of fractionation processes.

Relationship to Regional Suites

UNNAMED GRANITES AND THE TUNKILLIA SUITE

The unnamed granites exhibit strong spatial and temporal similarities to the Tunkillia Suite which is corroborated by geochemical and petrographical constraints.

U-Pb zircon analysis gives a weighted mean age of 1695±6 Ma. This is within error of the crystallisation ages given by (Payne et al., 2010; Ferris, 2004; Teasdale, 1997) of ~1670-1690 Ma for emplacement of the Tunkillia Suite.

Mineralogical similarities include a dominant mineralogy of quartz, K-feldspar, biotite and plagioclase with accessory minerals of zircon, apatite and titanite, as well as routinely displaying chloritized biotite and sericite alteration (Ferris, 2004; Payne et al., 2008).

The overall geochemistry of the unnamed granites and Tunkillia Suite are close to identical. They share fractional crystallisation trends displayed in variation diagrams (Fig.13), though, due to high content of SiO_2 and a low sample size, these trends are used cautiously. The fractional crystallisation trends are noticed as negative correlations between Al_2O_3, CaO, FeOt, MgO, TiO_2 and SiO_2 (Yanbo and Jingwen, 2010). This is supported by predominantly negative Eu/Eu* anomalies and depletions in Sr, P and Ti usually associated with feldspar controlled fractional crystallisation (Condie, 1989). Further geochemical similarities include moderately enriched LREE patterns, HREE traces that are relatively flat with some samples showing a more concave nature (Fig.14)

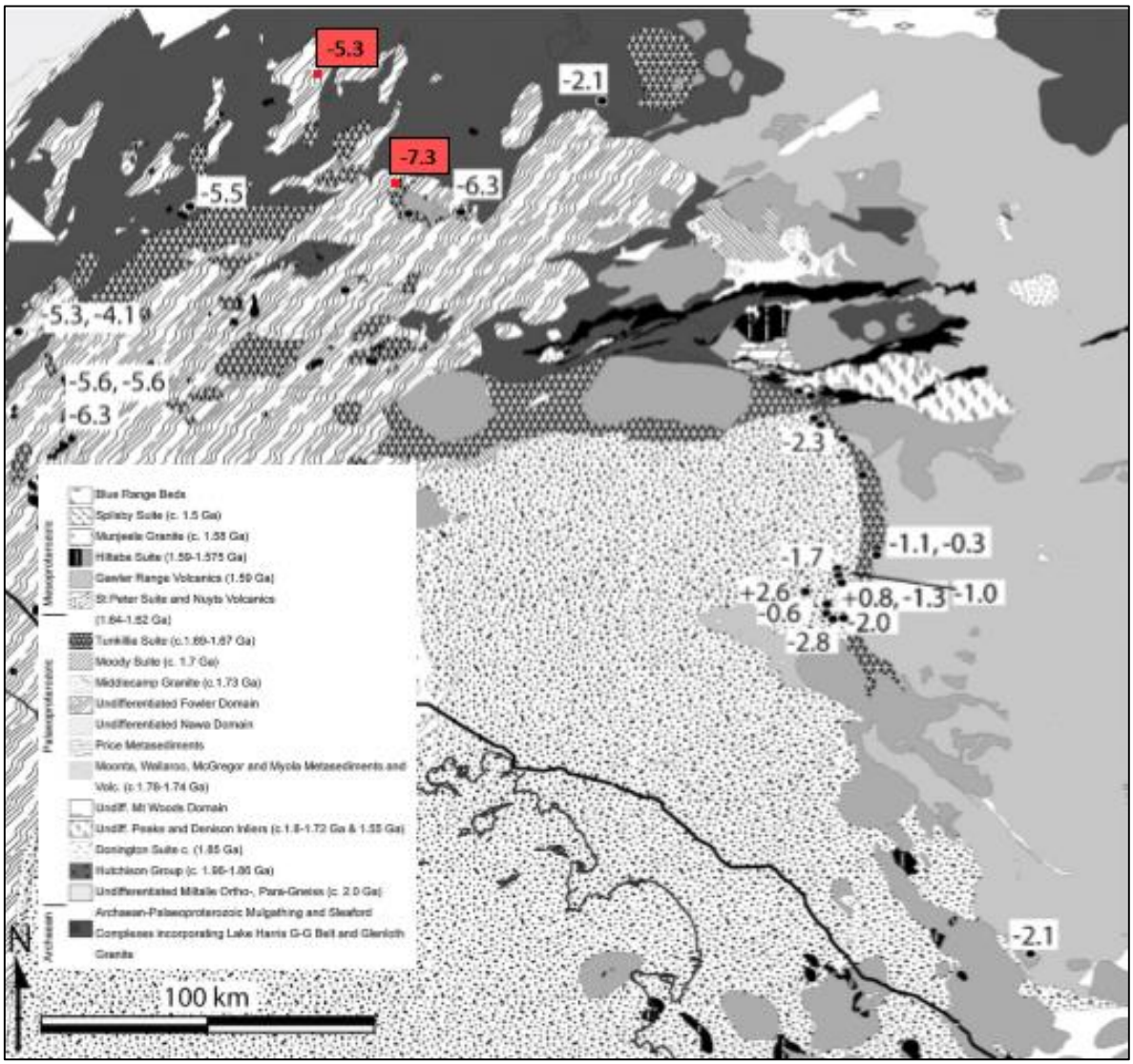

Figure 16: Distribution of εNd values for the Tunkillia suite modified from Payne et al. (2010) demonstrating the spatial variation between the eastern Tunkillia Suite and western Tunkillia Suite shown in white, and the continuation of this trend with the two unnamed granite samples shown in red.

and slightly positive Eu/Eu* anomalies. The unnamed granites and the Tunkillia Suite both plot predominantly within the volcanic arc, syn-collision and within-plate granite fields on Rb versus Y+Nb (Fig.12c,d). Using Frost et al. (2001) and Peccerillo and Taylor (1976) classification diagrams both are shown to be ferroan, high-K calc-alkalic to shoshonite and weakly peraluminous (Fig 10 and Fig 12a,b,e).

The megacrystic granite samples (306 and 307) produce $\varepsilon Nd_{(1695\ Ma)}$ = -5.3 and -7.2 which are spatially consistent with the western Tunkillia Suite. Payne et al. (2010) identified a spatial distribution where rocks that intrude the Christie and Fowler Domains consistently display εNd ~-5 to -6, while those in the eastern Tunkillia Suite are characteristically more juvenile. Initial Nd isotope values for the unnamed granites appear to correlate with this distribution pattern, fitting into the western Tunkillia Suite values. However, sample 307 (εNd -7.23) is comparatively more evolved than any Tunkillia sample and may represent a crustal melt end member for the Tunkillia Suite. This relationship can be seen in Figure 16 modified from Payne et al. (2010) showing the spatial distribution of epsilon Nd values for the Tunkillia Suite with the addition of the two unnamed granite samples.

LAKE ANTHONY GABBRO AND THE PETER PAN SUPERSUITE

U-Pb zircon geochronology for the Lake Anthony diorite indicate a magmatic crystallisation age of (1712±6 Ma). This is older than the Tunkillia Suite, however a similarly aged gabbros (Lzp1) have been identified in the Coober Pedy Ridge and the Olympic Dam deposit as a member of the Peter Pan SuperSuite (Wade and McAvaney, 2016). The Tunkillia Suite is also generally characterised by a lack of mafic or intermediate rocks (Payne et al., 2010) and therefore, is considered unsuited for comparison with the Lake Anthony gabbros.

U-Pb zircon geochronology conducted by Fanning et al. (2007) record ages of ~1725-1710 Ma for the Lzp1 gabbro which is within error for the Lake Anthony diorite sample and indicates an emplacement synchronous with the Kimban Orogeny (1730 – 1690 Ma; Hand et al., 2007). The Lake Anthony gabbro samples produce $\varepsilon Nd_{(1612\ Ma)} =$ -4.99 - -3.69, which are also to the Lzp1 gabbro $\varepsilon Nd_{(1620\ Ma)}$ = -5.9 - -4.6 (Fig.15).

Mineralogically the Lzp1 gabbro and the Lake Anthony gabbros are both fine to medium grained and are dominated by hornblende, plagioclase and biotite. Plagioclase crystals are observed in both suites and are randomly oriented and partially altered to sericite (Wade and McAvaney, 2016). Both show evidence of low-T thermal metamorphism with a lack of pyroxene, indicative of lower amphibolite facies conditions. Differences in mineralogy include interstitial quartz present in Lake Anthony samples but is a feature lacking in the Lzp1 gabbro.

Lake Anthony gabbros display a variation in REE and trace element abundances relative to Lzp1, with spider plots showing an overall enrichment in all REE's for the Lake Anthony samples (Fig. 14). The enriched patterns are similar to other mafic members of the Peter Pan SuperSuite, specifically the Colona Gabbro, a typically calc-alkaline metagabbro – granodiorite (Wade and McAvaney, 2016). The Colona Gabbro has similarly been subject to amphibolite facies metamorphism recorded at 1718±15 Ma (Reid, 2015). As previously mentioned Lake Anthony samples revealed similar metamorphic traits with a lack of pyroxene indicative of low – P, high – T conditions. This is consistent with metamorphic conditions of the Kimban Orogeny in the Christie Domain during the 1730 – 1700 Ma time period (Day et al., 1998). However, U-Pb zircon dating on the Colona Gabbro imply a crystallisation age of 1739±6 Ma (Reid, 2015), which is not reconcilable with the age of the Lake Anthony diorite

Constraints on Source Region

UNNAMED GRANITES

The two unnamed granites analysed show evolved Nd isotope values that fall completely within the Archean Mulgathing field (Fig.15), suggesting that the melt has been derived almost entirely from the Archean crust. All unnamed granites also show significant Nb and Ti depletions (Fig.14) which typically can be attributed to crustal assimilation and/or mixing with crust-derived magma (Rudnick and Gao, 2003) but also can suggest remelting of existing crust. This conclusion is supplemented by observations by Rudnick and Fountain (1995) stating granites resulting in melting of the crust should have high Th (>10 ppm), Pb (>20 ppm) and U (> 2.0 ppm) (Table 4). The presence of high La_n/Yb_n ratios displayed by the granites are also indicative of crustal composition (Taylor and McLennan, 1985)(Table 4).

Most samples display relatively enriched LREE and flat HREE patterns (Fig.14) and negative Eu/Eu* anomalies (Table 4) that are suggestive of plagioclase as a restite phase during the melting process (Taylor and McLennan, 1985). However, the megacrystic granite from near Edoldeh (Sample 306) displays a prominent positive a Eu/Eu* anomaly accompanied by a concave REE pattern indicating hornblende-rich restite phase (Payne et al., 2010). T_{DM} model age of ~2.5 Ga (Table 5) and suggested melting of the Archean crust suggest the protolith for the unnamed granites was most likely an Archean gneiss or amphibolite metamorphosed during the Sleaford Orogeny (Daly et al., 1998).

LAKE ANTHONY GABBROS

Nd isotope constraints of the Lake Anthony gabbros reveal the presence of crustal contamination and/or enriched mantle source region. The Lake Anthony samples have relatively evolved Nd isotope signatures (εNd = -3.4 - -4.9) and coupled with somewhat steep REE patterns (La_n/Yb_n = ~8 – 10; Table 4) that trend close to bulk crust abundances (Sun and McDonough, 1995), suggesting they may have been derived from an enriched lithospheric mantle source. La_n/Sm_n ratios provide a useful index for mantle source enrichment in magmas, with increasing enrichment relative to normal arc island basalts (2.39) (Hoatson et al., 2005). High La_n/Sm_n ratios for the Lake Anthony gabbros are between 2.7 and 3.4 (Table. 3) are consistent with an enriched lithospheric mantle interpretation. Contrastingly, the Lzp1 gabbro have lower La_n/Sm_n values of ~1.3, and exhibit overall REE patterns which indicate a comparatively juvenile mantle source (Fig.14). However, the Lzp1 gabbro display relatively evolved Nd signatures (~-5.9 - -4.6) suggesting that they have been modified (Wade and McAvaney, 2016). This may be due to enrichment of the mantle which enough can occur due to recycling of the continental lithosphere during subduction delamination of the lithosphere or by various types of mantle metasomatism (Zindler et al., 1979).

The varying nature between the depleted Lzp1 and the enriched Lake Anthony gabbros is consistent with findings by Wade and McAvaney (2016) when compared to other mafic units in the Peter Pan SuperSuite. They show the variances in geochemical signatures that contrast significantly between the enriched calc-alkaline amphibolites and depleted gabbros (Lzp1). This is possibly explained by a long lived heterogeneous mantle reservoir in the mid-Proterozoic identified by Schaefer (1998), whereby an older enriched lithospheric mantle and a younger juvenile mantle have been remelted during

the Kimban Orogeny (Wade and McAvaney, 2016). The Lake Anthony gabbros are likely derived from the older enriched lithospheric mantle based on their REE geochemical signatures.

TECTONIC IMPLICATIONS

UNNAMED GRANITES

The unnamed granites are identified as high-K calc-alkalic, which are typically thought to be generated in island arc and continental margin arcs associated with subductions zones (Peccerillo and Taylor, 1976; Condie, 1989). The affinity within volcanic arc settings is also seen when samples are plotted on Nb/Y and Rb/Y+Nb diagrams of (Pearce et al. 1984)(Fig.12c,d), which were used to initially classify the Tunkillia Suite as a subduction related granite (Betts and Giles, 2006). However, the application of such discrimination diagrams to Paleoproterozoic rocks is still debated, as they were defined using Phanerozoic rocks (Swain et al., 2008). Förster (1997) also remarks that differentiation in magma sources can produce compositional trends that cross field boundaries (a trend noticed in the unnamed granites). The unnamed granites are classed as ferroan on the Fe* diagram by Frost et al. (2001)(Fig.12a), these which can be construed to reflect an anorogenic origin, however, magnesian granites which are >70% SiO_2 are prone to transgress field boundaries which can misrepresent the classification (Frost et al., 2001).

As previously mentioned, the two unnamed granite samples measured for Sm – Nd have Nd isotope signatures that plot well within the local Archean basement (Fig.15), which must be taken into consideration. The geochemistry of the unnamed granites may be a reflection of the Archean source rock rather than the precipitants themselves (Frost et

al., 2001). This largely inhibits an unequivocal accurate assessment for a tectonic setting by geochemical constraints, which is compounded by a lack mafic end members in the unnamed granites as well as in the Tunkillia Suite (Payne et al. 2010). U-Pb geochronology of sample 307 reveals a crystallisation age of 1695±6 Ma which is towards the cessation of the Kimban Orogeny (~1690 Ma; Hand et al., 2007) invoking a classification of syn-late tectonic to best describe the unnamed granites.

LAKE ANTHONY GABBROS

The Lake Anthony samples plot wholly in the tholeiitic field on the AFM diagram (Fig.11). Generally tholeiitic mafic rocks are generated from upper-continental crustal levels as a result of decompression melting caused by lithospheric extension (Condie, 1989; Collins et al., 2016). Implicating the presence of extensional regimes for the Kimban Orogeny (Wade and McAvaney, 2016) which is synchronous with collisional and transpressional orogenesis (Teasedale, 1997; Hand et al., 2007; Payne et al., 2008). Therefore, a possible tectonic scenario for the Lake Anthony gabbros based on the evidence outlined above is emplacement in a back-arc extensional regime where subduction or metasomatic processes have enriched the mantle reservoir.

CONCLUSION

Geochronological, geochemical and petrological constraints have extended the knowledge of the two lithologies observed from BARTON and TALLARINGA regions. A combination of U-Pb zircon analysis, isotopic and geochemical data in conjunction with mineralogical similarities strongly suggest the unnamed granites are a member of the Tunkillia Suite. The tectonic setting of the unnamed granites remain relatively undefined due to limited isotope data as well as a lack of juvenile end members, however, timing of emplacement suggests a syn-late tectonic setting with respect to the Kimban Orogeny. Age constraints on The Lake Anthony gabbros reveal a synchronous emplacement with the Kimban Orogeny qualifying the gabbroic suite as an equivalent to mafic members of the Peter Pan SuperSuite. U-Pb zircon dating with REE and trace element data indicate the Lake Anthony gabbro are an enriched equivalent to the tholeiitic gabbro Lzp1. Geochemical constraints indicate an emplacement regime possibly in a back arc basin.

ACKNOWLEDGEMENTS

I would like to thank Professor Karin Barovich for her continual support and encouragement throughout the year. I am also indebted to Claire Wade and Stacey McAvaney from the Geological Survey of South Australia, of whom without their guidance this thesis would not have been possible. I would also like to show gratitude towards James Hall for help with field work and his exceptional digging skills. I give thanks to the efforts of Dr Katie Howard for laboratory training as well as making ongoing support available. Thanks go to David Bruce for the collecting and analysing of isotopic datasets. Furthermore, I would like to thank Professors Alan Collins and John Foden for a truly unforgettable tour of New Zealand and its incredible geology. Finally I must show appreciation and admiration to my Honours peers for their friendship and support throughout the year.

REFERENCES

Benbow, M. C. (1991). TALLARINGA, South Australia 1:250 000 geological series explanatory notes - sheet SH53-5.: Geological Survey of South Australia.

Betts, P. G., & Giles, D. (2006). The 1800–1100 Ma tectonic evolution of Australia. *Precambrian Research, 144*(1), 92-125

Boynton, W. V., & Henderson, P. (1984). Cosmochemistry of the Rare Earth Elements: Meteorite Studies *Developments in Geochemistry* (Vol. Volume 2, pp. 63-114): Elsevier.

Chappell, B. W. (1996). Magma Mixing and the Production of Compositional Variation within Granite Suites: Evidence from the Granites of Southeastern Australia. *37*(3), 449-470.

Collins, W. J., Huang, H.-Q., & Jiang, X. (2016). Water- fluxed crustal melting produces Cordilleran batholiths.(Author abstract). *44*(2), 143

Condie, K. C. (1989). *Plate tectonics & crustal evolution / by Kent C. Condie* (3rd ed. ed.). Oxford ; New York: Oxford ; New York : Pergamon Press.

Daly, S. J., Fanning, C.M. & Fairclough, M.C.,. (1998). Tectonic evolution and exploration potential of the Gawler Craton, South Australia. *AGSO Journal of Australian Geology and Geophysics, 17*(3), 145-168.

Dempster, T. J., Jenkin, G. R. T., & Rogers, G. (1994). The Origin of Rapakivi Texture. *Journal of Petrology, 35*(4), 963-981

Fanning, C. M., Flint, R. B., Parker, A. J., Blissett, K. R., & Ludwig, A. H. (1988). Refined Proterozoic evolution of the Gawler Craton, South Australia, through U-Pb zircon geochronology. *Precambrian Research, 40-41*(C), 363-386.

Fanning, C. M. a. (2007). *A geochronological framework for the Gawler Craton, South Australia / C.M. Fanning, A.J. Reid, G.S. Teale*: Adelaide : Mineral Resources Group, Division of Minerals and Energy Resources, Primary Industries and Resources South Australia.

Fenn, P. M. (1977). The nucleation and growth of alkali feldspars from hydrous melts (Vol. 15, pp. 135-161). Ottawa, ON: Ottawa, ON, Canada: Mineralogical Association of Canada.

Ferris, G. M., & Schwarz, M. (2004). *Definition of the Tunkillia Suite*: Mines and Energy South Australia, Parkside, South Australia.

Fraser, G., Reid, A., & Stern, R. (2012). Timing of deformation and exhumation across the Karari Shear Zone, north-western Gawler Craton, South Australia. *Australian Journal of Earth Sciences, 59*(4), 547-570.

Frost, B. R., Barnes, C. G., Collins, W. J., Arculus, R. J., Ellis, D. J., & Frost, C. D. (2001). A Geochemical Classification for Granitic Rocks. *Journal of Petrology, 42*(11), 2033-2048.

Förster, H. J., Tischendorf, G., & Trumbull, R. B. (1997). An evaluation of the Rb vs. (Y + Nb) discrimination diagram to infer tectonic setting of silicic igneous rocks. *Lithos, 40*(2), 261-293.

Hand, M., Reid, A., & Jagodzinski, L. (2007). Tectonic Framework and Evolution of the Gawler Craton, Southern Australia. *Economic Geology, 102*(8)

Hoatson, D. M. (2005). Late Archean Lake Harris Komatiite, Central Gawler Craton, South Australia:

Irvine, T. N., & Baragar, W. R. A. (1971). A Guide to the Chemical Classification of the Common Volcanic Rocks. *Canadian Journal of Earth Sciences, 8*(5), 523-548.

Jagodzinski, E.A. a. G. F. (2009). Compilation of SHRIMP U-Pb geochronological data for the Mulgathing Complex, Gawler Craton, South Australia, 2007–09.

Mahoney, J. J., & Coffin, M. F. (1997). *Large igneous provinces: continental, oceanic, and planetary flood volcanism / John J. Mahoney, Millard F. Coffin, editors*. Washington, DC: Washington, DC : American Geophysical Union.

McAvaney, S. (2012). The Cooyerdoo Granite: Paleo- and Mesoarchean basement of the Gawler Craton. *MESA Journal, 65*, 31-40.

McDonough, W. F., & Sun, S. s. (1995). The composition of the Earth. *Chemical Geology, 120*(3), 223-253.

McLean, M. A., & Betts, P. G. (2003). Geophysical constraints of shear zones and geometry of the Hiltaba Suite granites in the western Gawler Craton, Australia (Vol. 50, pp. 525-541). Oxford, UK.

Payne, J. L. (2008). Palaeo- to Mesoproterozoic evolution of the Gawler Craton, Australia: geochronological, geochemical and isotopic constraints. In K. M. Barovich & M. P. Hand (Eds.).

Payne, J. L., Ferris, G., Barovich, K. M., & Hand, M. (2010). Pitfalls of classifying ancient magmatic suites with tectonic discrimination diagrams: An example from the Paleoproterozoic Tunkillia

Suite, southern Australia. *Precambrian Research, 177*(3–4), 227-240. doi:http://dx.doi.org/10.1016/j.precamres.2009.12.005

Payne, J. L., Hand, M., Barovich, K. M., & Wade, B. P. (2008). Temporal constraints on the timing of high-grade metamorphism in the northern Gawler Craton: implications for assembly of the Australian Proterozoic. *Australian Journal of Earth Sciences, 55*(5), 623-640.

Pearce, J. A., Harris, N. B. W., & Tindle, A. G. (1984). Trace Element Discrimination Diagrams for the Tectonic Interpretation of Granitic Rocks. *Journal of Petrology, 25*(4), 956-983.

Peccerillo, A., & Taylor, S. R. (1976). Geochemistry of eocene calc- alkaline volcanic rocks from the Kastamonu area, Northern Turkey. *Contr. Mineral. and Petrol., 58*(1), 63-81.

Rankin, L. R. (1996).Explanatory notes for the BARTON mapsheet, South Australia : sheet SH53-9: Eastwood, S. Aust. : Mines and Energy South AustraliaReid, A. J. (2015). *Zircon U-pb geochronology from selected Paleopropterozoic igneous rocks of the Gawler Craton by laser ablation-inductively coupled plasma mass spectrometry* Retrieved from

Rudnick, R. L., & Fountain, D. M. (1994). Nature and composition of the continental crust; the view from down under (Vol. 75, pp. 72). Washington, DC: Washington, DC, United States: American Geophysical Union.

Rudnick, R. L., Gao, S., & Turekian, K. K. (2003). Composition of the Continental Crust *Treatise on Geochemistry* (pp. 1-64). Oxford: Pergamon.

Sandiford, M., McLaren, S., & Neumann, N. (2002). Long-term thermal consequences of the redistribution of heat-producing elements associated with large-scale granitic complexes. *Journal of Metamorphic Geology, 20*(1), 87-98.

Schaefer, B. F. (1998). Insights into Proterozoic tectonics from the southern Eyre Peninsula, South Australia / *Bruce F. Schaefer.*PhD thesis: 131

Schwarz, M. (1999). Definition of the Moody Suite, Southern Gawler Craton. *MESAJ, 013*, 033-044.

Shand, S. J. b. (1947). *Eruptive rocks : their genesis, composition, classification, and their relation to ore-deposits, with a chapter on meteorites* (3rd ed. ed.). Lond.: Lond. : Murby.

Sláma, J., Košler, J., Condon, D. J., Crowley, J. L., Gerdes, A., Hanchar, J. M., Whitehouse, M. J. (2008). Plešovice zircon — A new natural reference material for U– Pb and Hf isotopic microanalysis.*Chemical Geology, 249*(1-2), 1-35. doi:10.1016/j.chemgeo.2007.11.005

Stewart, J. R., & Betts, P. G. (2010a). Implications for Proterozoic plate margin evolution from geophysical analysis and crustal-scale modeling within the western Gawler Craton, Australia. *Tectonophysics, 483*(1–2), 151-177. doi:http://dx.doi.org/10.1016/j.tecto.2009.11.016

Swain, G., Barovich, K., Hand, M., Ferris, G., & Schwarz, M. (2008). Petrogenesis of the St Peter Suite, southern Australia: Arc magmatism and Proterozoic crustal growth of the South Australian Craton.*Precambrian Research, 166*(1–4), 283-296.

Teasdale, J. (1997). Methods for understanding poorly exposed terranes : the interpretive geology and tectonothermal evolution of the western Gawler Craton / Jonathan Teasdale.

Wade, B. P., Barovich, K. m., Hand, M., Scrimgeour, I. r., & Close, D. f. (2006). Evidence for Early Mesoproterozoic Arc Magmatism in the Musgrave Block, Central Australia: Implications for Proterozoic Crustal Growth and Tectonic Reconstructions of Australia. *The Journal of Geology, 114*(1), 43-63.

Wade, C. E., & McAvaney, S. O. (2016). *Geochemistry of the Peter Pan Supersuite.* Report Book 2016/0026. Department for State Development, South Australia, Adelaide.

Webb, A. W., Thomson, B. P., Blissett, A. H., Daly, S. J., Flint, R. B., & Parker, A. J. (1986). Geochronology of the Gawler Craton, South Australia. *Australian Journal of Earth Sciences, 33*(2), 119-143.

White, A. J. R. (1983). Granitoid types and their distribution in the Lachlan Fold Belt, southeastern Australia. In B. W. Chappell (Ed.), *In: Roddick, J.A (Ed). Circumpacific plutonic terrances* (Vol. 159, pp. 21-34): Geological society of America. Memoirs.

Yanbo, C., & Jingwen, M. (2010). Age and geochemistry of granites in Gejiu area, Yunnan province, SW China: Constraints on their petrogenesis and tectonic setting. *Lithos, 120*(3–4), 258-276.

Zindler, A., Hart, S. R., Frey, F. A., & Jakobsson, S. P. (1979). Nd and Sr isotope ratios and rare earth element abundances in Reykjanes Peninsula basalts evidence for mantle heterogeneity beneath Iceland.*Earth and Planetary Science Letters, 45*(2), 249-262.

APPENDIX A: U-PB ZIRCON GEOCHROLOGY DATA

Sample 307-Megatcrystic granite from Mobella Soak

	Isotope Ratios				Ages				
Analysis	Pb207/U235		Pb206/U238		Pb207/Pb206		Pb206/U238		Concordancy
307 - 1.d	4.252	0.084	0.2966	0.0039	1679	20	1678	37	100.0596
307 - 3.d	4.33	0.15	0.2952	0.0051	1672	24	1728	75	96.75926
307 - 5.d	4.059	0.095	0.2912	0.0045	1646	23	1650	54	99.75758
307 - 6.d	4.33	0.14	0.2996	0.0057	1688	28	1703	69	99.1192
307 - 7.d	4.29	0.13	0.3083	0.0048	1733	24	1663	57	104.2093
307 - 8.d	4.28	0.1	0.3004	0.0033	1692	16	1678	44	100.8343
307 - 12.d	4.07	0.15	0.2851	0.0065	1615	33	1682	79	96.01665
307 - 13.d	4.192	0.066	0.3003	0.0032	1694	16	1656	33	102.2947
307 - 14.d	4.42	0.13	0.3039	0.0047	1709	23	1729	61	98.84326
307 - 15.d	4.38	0.13	0.3021	0.0053	1702	26	1717	52	99.12638
307 - 16.d	4.19	0.17	0.298	0.0067	1678	33	1666	77	100.7203
307 - 18.d	4.28	0.1	0.2947	0.0045	1664	22	1714	48	97.08285
307 - 19.d	4.37	0.1	0.3041	0.0045	1710	22	1675	47	102.0896
307 - 20.d	4.38	0.14	0.3067	0.0048	1723	23	1653	61	104.2347
307 - 21.d	4.28	0.11	0.2934	0.0044	1662	22	1704	47	97.53521
307 - 22.d	4.314	0.076	0.3039	0.0039	1709	19	1666	33	102.581
307 - 23.d	4.279	0.061	0.3039	0.0036	1710	18	1664	31	102.7644
307 - 24.d	4.43	0.16	0.29	0.0056	1648	29	1782	72	92.48036
307 - 26.d	4.27	0.12	0.2958	0.0046	1671	23	1699	51	98.35197
307 - 27.d	4.41	0.14	0.2977	0.005	1678	25	1772	61	94.69526
307 - 30.d	4.37	0.16	0.2993	0.0064	1685	32	1704	76	98.88498
307 - 31.d	4.32	0.13	0.2936	0.0053	1660	26	1752	63	94.74886
307 - 33.d	4.412	0.086	0.3111	0.0037	1747	18	1674	44	104.3608
307 - 34.d	4.331	0.099	0.3034	0.0046	1707	23	1672	51	102.0933
307 - 35.d	4.12	0.15	0.2909	0.0058	1644	29	1684	74	97.6247
307 - 38.d	4.23	0.099	0.2966	0.0045	1676	22	1675	40	100.0597
307 - 39.d	4.332	0.078	0.3051	0.0038	1715	19	1666	36	102.9412
307 - 43.d	4.59	0.14	0.3045	0.0053	1714	26	1793	56	95.59398
307 - 44.d	4.38	0.13	0.298	0.005	1682	25	1724	59	97.56381
307 - 45.d	4.303	0.08	0.2903	0.003	1642	15	1756	36	93.50797
307 - 48.d	4.251	0.083	0.2995	0.0041	1690	20	1697	37	99.58751
307 - 50.d	4.34	0.11	0.3083	0.0043	1731	21	1670	44	103.6527
307 - 52.d	4.29	0.12	0.2959	0.0049	1674	25	1702	51	98.35488
307 - 53.d	4.309	0.076	0.3012	0.0034	1697	17	1675	36	101.3134
307 - 54.d	4.46	0.1	0.3103	0.0044	1741	22	1699	46	102.472
307 - 55.d	4.317	0.085	0.3019	0.0041	1699	20	1704	40	99.70657
307 - 56.d	4.312	0.096	0.3058	0.0041	1719	20	1660	43	103.5542
307 - 57.d	4.234	0.083	0.305	0.0035	1715	17	1618	39	105.9951
307 - 58.d	4.388	0.075	0.3023	0.0036	1704	18	1714	37	99.41657
307 - 59.d	4.5	0.12	0.3076	0.005	1727	25	1745	46	98.96848
307 - 60.d	4.54	0.11	0.2987	0.0058	1682	29	1779	43	94.5475
307 - 61.d	4.26	0.13	0.2961	0.0044	1671	22	1701	65	98.23633
307 - 62.d	4.323	0.07	0.3022	0.0037	1702	18	1682	36	101.1891
307 - 63.d	4.517	0.09	0.3144	0.0043	1763	21	1689	37	104.3813
307 - 65.d	4.141	0.091	0.2929	0.0044	1655	22	1701	40	97.29571
307 - 66.d	4.346	0.088	0.3072	0.0045	1730	22	1693	35	102.1855
307 - 67.d	4.283	0.08	0.298	0.004	1680	20	1702	37	98.7074
307 - 69.d	4.31	0.16	0.2953	0.006	1669	29	1715	76	97.31778
307 - 71.d	4.4	0.11	0.3036	0.004	1708	20	1721	36	99.24463
307 - 74.d	4.4	0.12	0.3102	0.0053	1740	26	1676	63	103.8186
307 - 75.d	4.33	0.096	0.3002	0.004	1691	20	1716	39	98.54312

	Isotope Ratios				Ages				
Analysis	Pb207/U235		Pb206/U238		Pb207/Pb206		Pb206/U238		Concordancy
307 - 77.d	4.294	0.093	0.3042	0.0041	1711	20	1682	45	101.7241
307 - 78.d	4.52	0.059	0.3167	0.0033	1773	16	1673	22	105.9773
307 - 79.d	4.344	0.08	0.3018	0.0047	1699	23	1721	30	98.72167
307 - 83.d	4.569	0.085	0.3079	0.0039	1733	19	1753	36	98.8591
307 - 84.d	4.489	0.053	0.3154	0.0034	1767	17	1682	16	105.0535
307 - 85.d	4.23	0.11	0.29	0.0049	1640	24	1726	46	95.01738
307 - 90.d	4.378	0.063	0.2982	0.0034	1683	17	1734	23	97.05882
307 - 92.d	4.069	0.062	0.2837	0.0033	1609	17	1684	28	95.54632
307 - 93.d	4.28	0.1	0.2934	0.0051	1657	25	1706	46	97.12778
307 - 94.d	4.08	0.18	0.2849	0.0062	1620	31	1628	79	99.5086
307 - 96.d	4.4	0.13	0.2957	0.0047	1673	23	1758	57	95.16496
307 - 99.d	4.26	0.12	0.2931	0.0045	1655	22	1719	59	96.27691
307 - 100.d	4.34	0.11	0.3027	0.0045	1703	22	1704	50	99.94131
307 - 101.d	4.15	0.15	0.2828	0.0052	1604	26	1707	67	93.96602
307 - 102.d	4.272	0.062	0.3021	0.0031	1701	16	1685	28	100.9496
307 - 103.d	4.4	0.13	0.3102	0.0056	1740	27	1705	64	102.0528
307 - 105.d	4.26	0.16	0.2994	0.006	1686	30	1708	76	98.71194
307 - 108.d	4.331	0.083	0.3096	0.004	1738	20	1661	38	104.6358
307 - 113.d	4.3	0.11	0.3081	0.0038	1732	19	1652	45	104.8426
307 - 115.d	4.34	0.13	0.3064	0.005	1724	24	1682	52	102.497
307 - 116.d	4.21	0.14	0.2913	0.0053	1646	26	1702	71	96.70975
307 - 117.d	4.43	0.14	0.306	0.0059	1719	29	1702	62	100.9988
307 - 118.d	4.06	0.15	0.296	0.0052	1672	26	1645	78	101.6413
307 - 119.d	4.15	0.15	0.2842	0.0059	1613	30	1688	71	95.55687
307 - 121.d	4.21	0.1	0.2989	0.0038	1685	19	1648	48	102.2451
307 - 122.d	4.46	0.12	0.303	0.0053	1705	26	1734	60	98.32757
307 - 123.d	4.39	0.14	0.3083	0.0058	1733	29	1679	65	103.2162
307 - 125.d	4.26	0.11	0.3048	0.0041	1714	20	1655	48	103.565
307 - 127.d	4.364	0.096	0.312	0.0042	1751	20	1649	43	106.1856
307 - 128.d	4.301	0.075	0.3001	0.0034	1691	17	1714	32	98.65811
307 - 130.d	4.2	0.15	0.2921	0.0054	1650	27	1701	66	97.00176
307 - 132.d	4.177	0.098	0.3024	0.004	1704	20	1658	44	102.7744
307 - 133.d	4.37	0.11	0.3047	0.0046	1713	23	1701	51	100.7055
307 - 134.d	4.12	0.1	0.2935	0.0043	1660	21	1649	50	100.6671
307 - 135.d	4.44	0.15	0.3014	0.0054	1696	27	1742	57	97.35936
307 - 136.d	4.348	0.095	0.3057	0.0043	1718	21	1659	36	103.5564
307 - 137.d	4.22	0.21	0.2843	0.008	1616	39	1739	98	92.92697
307 - 139.d	4.23	0.18	0.3015	0.0067	1696	33	1665	88	101.8619
307 - 140.d	4.293	0.088	0.2937	0.0038	1659	19	1738	37	95.45455
307 - 141.d	4.24	0.12	0.2991	0.0049	1685	24	1681	52	100.238
307 - 142.d	4.28	0.12	0.3024	0.0057	1704	28	1662	60	102.5271
307 - 144.d	4.35	0.1	0.3006	0.0044	1695	22	1734	41	97.75087
307 - 147.d	4.03	0.11	0.2889	0.005	1637	25	1649	54	99.27229
307 - 149.d	4.3	0.12	0.3047	0.0047	1716	23	1676	53	102.3866
307 - 150.d	4.38	0.14	0.3044	0.0045	1712	22	1714	60	99.88331
307 - 151.d	4.15	0.11	0.2892	0.005	1638	25	1703	61	96.18321
307 - 152.d	4.253	0.08	0.2989	0.0038	1685	19	1704	35	98.88498
307 - 154.d	4.23	0.13	0.2971	0.0049	1675	24	1688	67	99.22986
307 - 155.d	4.315	0.081	0.3004	0.0034	1692	17	1681	36	100.6544
307 - 156.d	4.17	0.15	0.2962	0.0064	1673	32	1651	73	101.3325
307 - 158.d	4.41	0.13	0.3059	0.0061	1720	30	1685	58	102.0772
307 - 159.d	4.34	0.12	0.2924	0.0046	1652	23	1777	55	92.96567
307 - 160.d	4.48	0.092	0.3024	0.0047	1706	23	1748	40	97.59725

Sample 514 – Lake Anthony Diorite

	Isotope Ratios				Ages				
Analysis	Pb207/U235		Pb206/U238		Pb207/Pb206		Pb206/U238		Concordancy
514 - 162.d	4.754	0.081	0.326	0.0057	1820	28	1735	24	104.8991
514 - 4.d	4.625	0.057	0.3186	0.0029	1784	14	1702	21	104.8179
514 - 39.d	4.567	0.081	0.3177	0.0036	1778	18	1699	33	104.6498
514 - 42.d	4.68	0.1	0.3221	0.0043	1799	21	1721	41	104.5322
514 - 48.d	4.652	0.053	0.3202	0.0035	1790	17	1713	24	104.495
514 - 47.d	4.5	0.069	0.3154	0.004	1766	19	1693	27	104.3119
514 - 124.d	4.726	0.067	0.3219	0.0035	1798	17	1724	30	104.2923
514 - 202.d	4.34	0.11	0.3091	0.0044	1735	22	1664	45	104.2668
514 - 101.d	4.626	0.07	0.3184	0.0028	1782	14	1710	24	104.2105
514 - 64.d	4.703	0.086	0.319	0.0049	1783	24	1714	29	104.0257
514 - 212.d	4.324	0.086	0.3072	0.0035	1726	17	1660	40	103.9759
514 - 86.d	4.67	0.11	0.3186	0.0053	1792	25	1724	33	103.9443
514 - 210.d	4.583	0.075	0.3158	0.0032	1769	16	1703	32	103.8755
514 - 99.d	4.621	0.098	0.3178	0.0033	1778	16	1714	36	103.734
514 - 227.d	4.222	0.099	0.3037	0.0039	1712	20	1653	42	103.5693
514 - 61.d	4.567	0.062	0.3163	0.0035	1771	17	1710	20	103.5673
514 - 94.d	4.67	0.1	0.3176	0.0044	1781	21	1720	41	103.5465
514 - 36.d	4.32	0.051	0.3059	0.0026	1720	13	1662	18	103.4898
514 - 97.d	4.524	0.076	0.3142	0.0038	1760	18	1701	30	103.4685
514 - 166.d	5.053	0.081	0.3321	0.0041	1850	20	1793	30	103.179
514 - 14.d	4.291	0.086	0.3047	0.004	1714	20	1662	35	103.1288
514 - 222.d	4.315	0.048	0.3057	0.0027	1719	13	1667	19	103.1194
514 - 127.d	4.487	0.068	0.3125	0.0037	1754	18	1701	32	103.1158
514 - 117.d	4.436	0.086	0.3083	0.0036	1732	18	1680	35	103.0952
514 - 1.d	4.637	0.079	0.3168	0.0035	1775	17	1723	37	103.018
514 - 63.d	4.438	0.097	0.3117	0.0045	1748	22	1698	39	102.9446
514 - 191.d	4.768	0.082	0.3227	0.0038	1802	19	1753	30	102.7952
514 - 98.d	4.371	0.059	0.307	0.0026	1726	13	1680	25	102.7381
514 - 229.d	4.62	0.12	0.3155	0.0037	1769	18	1722	41	102.7294
514 - 194.d	4.438	0.056	0.3099	0.0032	1741	15	1695	22	102.7139
514 - 87.d	4.299	0.055	0.3034	0.0026	1708	13	1663	21	102.706
514 - 29.d	4.318	0.098	0.3059	0.0044	1719	22	1674	43	102.6882
514 - 80.d	4.28	0.081	0.3016	0.0033	1698	16	1654	34	102.6602
514 - 183.d	4.44	0.1	0.3098	0.0042	1741	21	1697	47	102.5928
514 - 15.d	4.438	0.061	0.3085	0.0033	1733	16	1690	30	102.5444
514 - 142.d	4.408	0.06	0.3078	0.0033	1730	16	1688	23	102.4882
514 - 81.d	4.46	0.072	0.3116	0.0033	1748	16	1706	27	102.4619
514 - 146.d	4.296	0.057	0.3027	0.0032	1704	16	1666	22	102.2809
514 - 120.d	4.324	0.047	0.3053	0.0027	1717	13	1680	18	102.2024
514 - 11.d	4.348	0.071	0.3046	0.0033	1715	16	1679	31	102.1441
514 - 119.d	4.362	0.079	0.305	0.0034	1717	17	1681	33	102.1416
514 - 197.d	4.396	0.095	0.3063	0.0041	1725	20	1689	39	102.1314
514 - 76.d	4.451	0.058	0.3095	0.0033	1738	16	1703	25	102.0552
514 - 7.d	4.21	0.064	0.3001	0.0026	1691	13	1657	29	102.0519
514 - 185.d	4.39	0.1	0.3062	0.004	1721	20	1687	43	102.0154
514 - 5.d	4.443	0.085	0.3098	0.0039	1739	19	1705	41	101.9941
514 - 150.d	4.388	0.036	0.3065	0.0024	1723	12	1690	16	101.9527
514 - 69.d	4.309	0.045	0.303	0.0025	1706	12	1675	21	101.8507
514 - 167.d	4.515	0.077	0.3119	0.0035	1749	17	1722	28	101.5679
514 - 79.d	4.505	0.049	0.3101	0.0029	1740	14	1714	20	101.5169
514 - 44.d	4.604	0.093	0.3132	0.0043	1756	21	1733	42	101.3272
514 - 59.d	4.66	0.11	0.3147	0.0045	1763	22	1741	46	101.2636
514 - 165.d	4.62	0.13	0.3149	0.0047	1763	23	1743	47	101.1474

	Isotope Ratios				Ages				
Analysis	Pb207/U235		Pb206/U238		Pb207/Pb206		Pb206/U238		Concordancy
514 - 135.d	4.61	0.1	0.311	0.0041	1745	20	1726	39	101.1008
514 - 24.d	4.381	0.048	0.3051	0.0024	1717	11	1699	19	101.0594
514 - 129.d	4.678	0.081	0.3155	0.0047	1768	23	1751	22	100.9709
514 - 130.d	4.45	0.14	0.3045	0.0044	1713	22	1697	54	100.9428
514 - 68.d	4.44	0.12	0.3084	0.0045	1734	23	1718	50	100.9313
514 - 123.d	4.618	0.086	0.3121	0.0035	1750	17	1734	35	100.9227
514 - 159.d	4.327	0.06	0.3039	0.0027	1710	13	1695	24	100.885
514 - 174.d	4.413	0.064	0.3053	0.0031	1717	15	1705	25	100.7038
514 - 143.d	4.422	0.054	0.3067	0.0031	1724	15	1712	22	100.7009
514 - 10.d	4.786	0.087	0.3189	0.0041	1786	20	1774	36	100.6764
514 - 35.d	4.815	0.093	0.3193	0.0038	1786	19	1774	35	100.6764
514 - 23.d	4.424	0.091	0.3043	0.0034	1712	17	1701	38	100.6467
514 - 208.d	4.466	0.093	0.3079	0.0034	1732	16	1723	36	100.5223
514 - 201.d	4.501	0.079	0.3094	0.003	1737	15	1728	37	100.5208
514 - 126.d	4.291	0.065	0.2999	0.0029	1690	14	1682	30	100.4756
514 - 32.d	4.539	0.062	0.3091	0.0033	1736	16	1728	24	100.463
514 - 34.d	4.257	0.057	0.2984	0.0027	1683	13	1676	22	100.4177
514 - 90.d	4.293	0.051	0.2999	0.0024	1690	12	1683	21	100.4159
514 - 43.d	4.291	0.055	0.3003	0.0029	1694	14	1687	22	100.4149
514 - 93.d	4.36	0.11	0.3062	0.0042	1721	21	1714	42	100.4084
514 - 52.d	4.307	0.051	0.3017	0.003	1699	15	1693	21	100.3544
514 - 221.d	4.501	0.089	0.3089	0.0042	1734	21	1729	38	100.2892
514 - 184.d	4.363	0.088	0.3034	0.0038	1709	19	1706	35	100.1758
514 - 82.d	4.697	0.091	0.3138	0.0043	1759	21	1756	35	100.1708
514 - 19.d	4.83	0.12	0.3214	0.0053	1795	26	1792	32	100.1674
514 - 3.d	4.345	0.067	0.2994	0.0028	1690	14	1690	29	100
514 - 139.d	4.63	0.1	0.3121	0.0051	1750	25	1753	40	99.82886
514 - 220.d	4.612	0.076	0.3123	0.0039	1751	19	1756	18	99.71526
514 - 152.d	4.256	0.079	0.2988	0.0032	1688	16	1693	36	99.70467
514 - 104.d	4.49	0.059	0.3074	0.0026	1727	13	1733	21	99.65378
514 - 71.d	4.444	0.052	0.3055	0.0025	1719	13	1728	23	99.47917
514 - 50.d	4.323	0.055	0.2991	0.0026	1686	13	1695	20	99.46903
514 - 13.d	4.355	0.094	0.3	0.0037	1692	18	1702	43	99.41246
514 - 103.d	4.259	0.052	0.2976	0.0031	1680	15	1692	25	99.29078
514 - 209.d	4.4	0.12	0.3025	0.0043	1705	22	1718	49	99.24331
514 - 8.d	4.281	0.081	0.2998	0.005	1694	24	1707	43	99.23843
514 - 145.d	4.304	0.081	0.2984	0.0037	1684	19	1698	40	99.1755
514 - 199.d	4.614	0.094	0.3142	0.0043	1760	21	1775	43	99.15493
514 - 66.d	4.441	0.05	0.3052	0.0029	1718	14	1733	23	99.13445
514 - 85.d	4.314	0.078	0.3007	0.0036	1696	17	1713	39	99.00759
514 - 156.d	4.343	0.064	0.3	0.0029	1691	15	1708	27	99.00468
514 - 128.d	4.553	0.085	0.3061	0.0036	1721	18	1740	33	98.90805
514 - 187.d	4.79	0.11	0.3172	0.0035	1775	17	1795	42	98.88579
514 - 217.d	4.82	0.13	0.316	0.0048	1771	23	1791	51	98.88331
514 - 58.d	4.41	0.065	0.3024	0.0038	1703	19	1724	27	98.7819
514 - 140.d	4.415	0.059	0.303	0.0029	1706	14	1732	26	98.49885
514 - 215.d	4.545	0.089	0.3065	0.004	1723	20	1750	31	98.45714
514 - 121.d	4.879	0.083	0.3174	0.0036	1776	18	1804	34	98.44789
514 - 170.d	4.57	0.09	0.3088	0.0041	1734	20	1763	37	98.35508
514 - 189.d	4.239	0.08	0.2959	0.003	1671	15	1699	38	98.35197
514 - 195.d	4.71	0.11	0.3103	0.0045	1744	22	1780	47	97.97753
514 - 230.d	4.45	0.074	0.3015	0.0038	1698	19	1736	29	97.81106
514 - 225.d	4.45	0.11	0.3032	0.0041	1706	21	1745	46	97.76504
514 - 53.d	4.466	0.085	0.3017	0.0036	1703	17	1742	35	97.76119
514 - 18.d	4.083	0.072	0.2888	0.0038	1640	18	1680	34	97.61905
514 - 161.d	4.51	0.11	0.3062	0.0051	1721	25	1763	38	97.6177

	Isotope Ratios				Ages				
Analysis	Pb207/U235		Pb206/U238		Pb207/Pb206		Pb206/U238		Concordancy
514 - 25.d	4.47	0.11	0.3025	0.0054	1703	27	1748	39	97.42563
514 - 56.d	4.494	0.098	0.3037	0.0042	1709	21	1756	32	97.32346
514 - 105.d	4.487	0.071	0.3027	0.0036	1704	18	1753	19	97.20479
514 - 137.d	4.51	0.1	0.3021	0.0034	1701	17	1752	43	97.08904
514 - 115.d	4.61	0.1	0.3052	0.0049	1716	24	1776	47	96.62162
514 - 83.d	4.336	0.074	0.2964	0.003	1673	15	1733	30	96.5378
514 - 78.d	4.49	0.11	0.3002	0.0048	1691	24	1757	49	96.2436
514 - 114.d	4.395	0.083	0.296	0.0034	1671	17	1737	36	96.20035
514 - 125.d	4.314	0.069	0.2925	0.0038	1655	19	1721	33	96.16502
514 - 30.d	4.35	0.11	0.2941	0.0045	1664	22	1734	49	95.96309
514 - 75.d	4.56	0.093	0.303	0.004	1708	20	1781	31	95.90118
514 - 153.d	4.67	0.13	0.3056	0.0056	1722	28	1798	42	95.77308
514 - 46.d	4.61	0.13	0.3056	0.0054	1720	27	1797	53	95.71508
514 - 16.d	4.7	0.11	0.3084	0.0037	1732	18	1810	42	95.69061
514 - 190.d	4.97	0.13	0.3165	0.0043	1772	21	1855	42	95.52561
514 - 27.d	4.241	0.097	0.2893	0.004	1637	20	1715	47	95.4519
514 - 160.d	5.11	0.12	0.3189	0.0038	1785	18	1871	39	95.40353
514 - 33.d	4.41	0.12	0.2971	0.0049	1676	25	1757	44	95.38987

Sample 306 – Megacrystic granite from near Eldodeh Rock Hole

Contaminated by common lead (^{204}Pb)

	Isotope Ratios				Ages				
Analysis	Pb207/U235		Pb206/U238		Pb207/Pb206		Pb206/U238		Concordancy
306 - 1.d	5.92	0.24	0.3101	0.0086	1736	42	2220	83	127.8802
306 - 2.d	4.34	0.19	0.296	0.0064	1669	32	1731	79	103.7148
306 - 3.d	4.29	0.19	0.2871	0.0074	1627	37	1786	84	109.7726
306 - 4.d	4.7	0.14	0.3043	0.0044	1711	22	1826	65	106.7212
306 - 5.d	5.94	0.27	0.3079	0.0088	1726	43	2231	86	129.2584
306 - 6.d	4.2	0.2	0.2957	0.006	1672	30	1728	96	103.3493
306 - 7.d	4.11	0.18	0.2946	0.0073	1661	36	1667	83	100.3612
306 - 8.d	4.6	0.23	0.2927	0.0089	1654	45	1850	110	111.8501
306 - 9.d	6.3	0.33	0.2999	0.0081	1690	41	2353	92	139.2308
306 - 10.d	4.22	0.14	0.2908	0.0058	1643	29	1720	62	104.6865
306 - 11.d	4.44	0.21	0.284	0.0082	1611	41	1874	88	116.3253
306 - 12.d	4.27	0.16	0.293	0.0066	1657	33	1755	73	105.9143
306 - 13.d	4.35	0.21	0.3001	0.0084	1692	41	1700	100	100.4728
306 - 14.d	20.9	1.6	0.416	0.013	2245	59	3683	77	164.0535
306 - 15.d	4.4	0.19	0.2954	0.0074	1678	37	1786	88	106.4362
306 - 16.d	4.58	0.21	0.2964	0.0078	1674	39	1848	95	110.3943
306 - 17.d	4.64	0.28	0.2929	0.0089	1659	44	1880	120	113.3213
306 - 18.d	4.54	0.27	0.3068	0.0098	1724	48	1730	120	100.348
306 - 19.d	11.84	0.49	0.349	0.01	1924	49	3172	61	164.8649
306 - 20.d	4.49	0.22	0.2947	0.0073	1665	37	1815	97	109.009
306 - 21.d	4.25	0.25	0.2858	0.0098	1615	49	1770	110	109.5975
306 - 22.d	4.32	0.17	0.2978	0.0066	1678	33	1721	78	102.5626
306 - 23.d	4.99	0.32	0.2918	0.0097	1650	49	1990	120	120.6061
306 - 24.d	6.24	0.39	0.3094	0.0088	1737	43	2210	100	127.2309
306 - 25.d	4.63	0.23	0.2949	0.0083	1662	41	1816	98	109.2659
306 - 26.d	4.86	0.29	0.2901	0.009	1641	44	1960	110	119.4394
306 - 27.d	4.44	0.24	0.2888	0.0086	1636	44	1800	100	110.0244
306 - 28.d	4.14	0.26	0.2889	0.0081	1638	40	1650	130	100.7326

	Isotope Ratios				Ages				
Analysis	**Pb207/U235**		**Pb206/U238**		**Pb207/Pb206**		**Pb206/U238**		**Concordancy**
306 - 29.d	17.2	2.1	0.391	0.019	2106	85	3350	160	159.0693
306 - 30.d	4.42	0.17	0.3022	0.0063	1700	31	1728	62	101.6471
306 - 31.d	4.73	0.28	0.2951	0.0088	1663	44	1890	110	113.65
306 - 32.d	6.98	0.38	0.2985	0.0081	1683	41	2539	99	150.8616
306 - 33.d	28.5	1.8	0.448	0.015	2390	68	4085	59	170.9205
306 - 34.d	4.16	0.15	0.2888	0.0056	1634	28	1671	69	102.2644
306 - 35.d	5.1	0.21	0.2723	0.0066	1550	33	1975	57	127.4194
306 - 36.d	5.04	0.28	0.288	0.0074	1628	37	1990	100	122.2359
306 - 37.d	4.42	0.19	0.2894	0.006	1643	30	1773	81	107.9124
306 - 38.d	4.08	0.12	0.2907	0.0048	1643	24	1632	53	99.33049
306 - 39.d	4.79	0.23	0.3021	0.0082	1697	41	1839	88	108.3677
306 - 40.d	4.25	0.2	0.2947	0.0071	1661	35	1694	98	101.9868
306 - 41.d	4.74	0.21	0.2953	0.0078	1668	38	1899	89	113.8489
306 - 42.d	4.69	0.26	0.2888	0.009	1639	45	1880	110	114.7041
306 - 43.d	4.82	0.17	0.2783	0.0053	1581	27	1963	67	124.1619
306 - 44.d	4.56	0.24	0.2896	0.0099	1646	51	1820	120	110.5711
306 - 45.d	5.68	0.53	0.295	0.01	1661	51	2150	150	129.4401
306 - 46.d	4.58	0.18	0.2977	0.0061	1681	30	1795	83	106.7817
306 - 47.d	6.07	0.36	0.3044	0.009	1714	45	2233	94	130.28
306 - 48.d	4.77	0.24	0.2866	0.0083	1620	42	1922	94	118.642
306 - 49.d	3.96	0.16	0.2667	0.0067	1527	35	1723	84	112.8356
306 - 50.d	4.28	0.16	0.2867	0.0063	1626	31	1752	78	107.7491
306 - 51.d	23	1.2	0.424	0.013	2270	57	3853	57	169.7357
306 - 52.d	3.83	0.11	0.2542	0.0045	1459	23	1581	51	108.3619
306 - 53.d	7.16	0.33	0.3143	0.007	1759	34	2493	73	141.7283
306 - 54.d	4.19	0.25	0.2858	0.0083	1620	41	1649	99	101.7901
306 - 55.d	12.1	1.1	0.3409	0.0095	1886	46	3100	120	164.369
306 - 56.d	4.54	0.2	0.2894	0.007	1636	35	1834	94	112.1027
306 - 57.d	5.76	0.26	0.3258	0.0089	1820	42	2000	72	109.8901
306 - 58.d	9.37	0.71	0.33	0.01	1831	48	2737	98	149.4812
306 - 59.d	4.41	0.21	0.2823	0.0066	1607	34	1822	93	113.379
306 - 60.d	5.31	0.22	0.2896	0.006	1641	30	2069	91	126.0817

APPENDIX B: GEOCHEMISTRY OF REFERENCE SOURCES

Major and trace geochemistry from Payne et al. 2010 and UnpubGSSA data

Sample	Suite	SiO2	Al2O3	Fe2O3	CaO	MgO	Na2O	K2O	TiO2	MnO	P2O5	LOI
350424	Tunkillia	72	14.9	1.73	1.64	0.36	4.22	4.15	0.21	0.05	0.13	1.11
350426	Tunkillia	62.9	19.3	2.43	1.1	0.3	4.16	8.24	0.22	0.06	0.09	1.33
350427	Tunkillia	71.8	13.5	2.72	1.01	0.34	2.64	5.84	0.31	0.06	0.11	1.31
350428	Tunkillia	76.4	11.5	1.47	0.45	0.13	2.72	5.41	0.14	0.03	0.04	0.73
350429	Tunkillia	76.8	12	1.36	0.55	0.14	3.85	4.42	0.11	0.07	0.03	0.56
350431	Tunkillia	76.3	12.3	1.31	0.64	0.15	3.87	4.5	0.11	0.06	0.03	0.92
350433	Tunkillia	73.7	13.2	0.9	0.55	0.13	2.93	6.69	0.14	0.03	0.04	1.11
363434	Tunkillia	70.5	14.7	2.67	2.32	0.5	3.7	3.7	0.22	0.11	0.11	1.33
363435	Tunkillia	67.7	15.6	2.84	1.95	0.71	3.21	6.05	0.49	0.09	0.13	1.43
363436	Tunkillia	71.6	13.7	2.92	1.74	0.57	2.63	5.16	0.3	0.08	0.08	1.44
WGC165	Tunkillia	71.9	14.3	2.04	1.67	0.51	3.39	4.7	0.225	0.06	0.07	0.77
378933	Tunkillia	75.6	12.2	1.36	0.68	0.15	2.96	5.3	0.1	0.04	0.18	0.64
1840691	Tunkillia	65.4	15.95	4.342	1.97	1.02	4.16	4.92	0.56	0.09	0.269	0.58
370928	Tunkillia	72.9	11.9	5.14	0.26	0.09	2.13	5.23	0.17	0.005	0.02	1.65
370929	Tunkillia	75.6	12.8	1.99	0.36	0.17	2.13	6.58	0.2	0.04	0.03	0.85
370932	Tunkillia	68.9	14	5.11	2.63	1.34	3.07	3.7	0.64	0.16	0.12	1.05
370934	Tunkillia	75.3	12.9	2.11	0.18	0.14	2.86	6.36	0.2	0.01	0.03	0.54
370935	Tunkillia	76	13.1	0.85	0.31	0.12	2.95	6	0.11	0.02	0.08	0.68
370936	Tunkillia	77.1	12	1.62	0.64	0.21	2.91	4.73	0.14	0.08	0.03	0.77
444829	Tunkillia	70.645	14.63	3.255	1.545	0.859	3.447	4.573	0.546	0.03	0.046	0.134
444830	Tunkillia	70.04	15.05	2.62	2.21	0.67	3.148	5.54	0.316	0.03	0.095	0.159
879-47	Tunkillia	72.1	13.8	2.12	1.91	0.58	3.15	4.46	0.335	0.02	0.1	1.18
444828	Tunkillia	76.068	13.467	1.74	2.425	0.546	3.622	2.262	0.226	0.038	0.077	0.671
444831	Tunkillia	70.208	17.171	1.798	2.998	0.621	5.495	1.226	0.199	0.023	0.017	0.019
879-29B	Tunkillia	69.8	15.9	2.17	3.1	0.95	5.24	1.13	0.33	0.03	0.11	1.67
444832	Tunkillia	72.83	12.86	2.76	1.05	0.59	2.072	6.52	0.403	0.059	0.049	0.582
444833	Tunkillia	71.39	14.28	2.32	0.56	0.22	3.255	6.53	0.208	0.041	0.109	0.945
444834	Tunkillia	75.711	13.01	1.278	1.05	0.278	3.802	4.4	0.222	0.021	0.033	0.023
444835	Tunkillia	75.9	13.1	0.87	0.78	0.03	3.13	5.57	0.05	0.005	0.08	0.3
387418	Tunkillia	70.03	14.84	2.27	1	0.67	2.68	5.18	0.3	0.09	0.04	0
387427	Tunkillia	61.03	15.89	5.09	6.19	1.92	2.74	3.3	0.38	0.16	0.17	0
387429	Tunkillia	73.68	9.56	3.96	1.76	0.51	1.59	3.13	0.13	0.05	0.04	0
387431	Tunkillia	71.87	13.79	1.64	1.75	0.49	2.95	4.05	0.19	0.08	0.07	0
469565	Tunkillia	72.2	13.06	1.82	2.17	0.54	2	4.32	0.2	0.07	0.08	0
469566	Tunkillia	67.57	15.5	2.3	2.05	0.63	3.18	4.68	0.24	0.11	0.09	0
469567	Tunkillia	67.99	13.88	3.65	2.42	1.08	1.15	4.18	0.48	0.18	0.12	0
469568	Tunkillia	68.61	13.82	2.26	2.95	0.56	2.72	4.53	0.21	0.11	0.09	0
469569	Tunkillia	69.45	13.58	2.48	2.46	0.53	2.81	5.5	0.32	0.06	0.1	0
469570	Tunkillia	69.02	14.26	2.64	1.78	0.56	2.67	5.54	0.33	0.06	0.09	0
368571	Tunkillia	66.7	14.6	4.14	2.58	0.95	1.96	4.98	0.51	0.14	0.14	3.31
368573	Tunkillia	72.7	14.3	1.3	1.78	0.3	3.44	4.43	0.13	0.05	0.04	0.68
378920	Tunkillia	72.2	15	1.74	2.14	0.37	3.54	4.21	0.16	0.05	0.07	0.5
378921	Tunkillia	74.6	13.5	1.29	1.15	0.16	3.37	5.26	0.14	0.02	0.17	0.46
378924	Tunkillia	73	14.2	1.72	2.15	0.39	3.36	3.95	0.17	0.05	0.13	0.56
1840692	Tunkillia	75.04	12.33	1.714	0.6	0.26	3.33	5.425	0.22	0.08	0.036	0.32
1840702	Tunkillia	73.14	13.14	2.347	1.37	0.6	2.92	5.223	0.37	0.04	0.08	0.39
WGC81	Tunkillia	73.1	12.5	2.42	1.41	0.59	3.03	4.77	0.355	0.04	0.08	0.68
Christie1	Tunkillia	72.8	14.9	0	1.46	0.17	4.28	4.02	0.11	0.01	0.02	0.56
350435	Tunkillia	71	14.5	2.42	0.72	0.62	3.94	4.77	0.23	0.08	0.1	1.55
370933	Tunkillia	76.9	12.4	0.76	0.31	0.05	2.62	6.51		-0.01	0.01	0.66
370937	Tunkillia	75.1	12.6	1.31	0.22	0.18	2.97	6.15		0.03	0.03	0.49
370938	Tunkillia	72.9	13.1	3.32	0.57	0.45	3.03	5.93		0.05	0.07	0.32
1948337	Lzp1	40.52	13.09	24.11	9.92	6.47	1.98	0.35	3.67	0.22		
1948338	Lzp1	41.32	13.53	22.86	8.85	6.92	2.04	0.38	3.63	0.22		
1948339	Lzp1	41.99	13.43	22.23	10.58	6.83	2.05	0.34	3.5	0.22		
1948341	Lzp1	42.1	13.81	21.86	10.48	6.72	2.14	0.4	3.45	0.21		
1948342	Lzp1	40.1	12.29	23.72	11.15	6.71	1.85	0.38	4	0.21		
1948343	Lzp1	42.06	12.69	21.56	10.8	7.31	1.92	0.38	3.41	0.21		
1948344	Lzp1	41.14	13.68	20.56	10.3	6.48	2.06	0.49	3.67	0.21		
1948345	Lzp1	49.31	20.95	8.18	9.35	4.81	2.98	1.37	1	0.13		

Sample	Suite	Ba	Ce	Cs	Dy	Er	Eu	Gd	Ho	La	Lu	Nb	Nd	Pr	Rb	Sm	Sr	Th	U	Y	Yb	Zr
350424	**Tunkillia**	1250	46.5		2.9	1.9	1.1	3.1	0.6	26	0.4	8	19	5.5	120	3.2	360	13	3.3	15	2.3	140
350426	**Tunkillia**	600	27		2.6	1.5	0.8	1.9	0.5	15	0.2	14	13	3.4	410	2.5	58	22.5	3.9	11	1.6	160
350427	**Tunkillia**	460	98		6.5	3.5	0.8	5.5	1.1	48	0.5	13	44.5	11.5	300	8.5	54	27.5	5.5	31.5	3.5	120
350428	**Tunkillia**	270	140		8	4.3	0.6	6.5	1.4	78	0.6	11	60	16	230	10.5	35.5	26	4.7	35	4.3	140
350429	**Tunkillia**	200	60		7.5	4.6	0.4	4.8	1.4	25.5	0.8	23.5	29.5	7.5	250	7	43	41	6.5	38.5	5.5	120
350431	**Tunkillia**	220	70		7.5	4.6	0.4	5	1.4	30	0.7	26.5	33.5	8.5	270	8	41	26	4.8	41	5.5	130
350433	**Tunkillia**	1400	60		1.7	0.8	1.2	2.5	0.3	30.5	0.1	6	21.5	6.5	145	3.3	145	10	0.7	7	0.8	170
363434	**Tunkillia**	2250	56		1.7	0.9	1.9	2.4	0.3	33	0.2	6	21.5	6.5	72	2.8	500	3.1	0.4	8	0.9	180
363435	**Tunkillia**	2950	88		2.4	1.3	2.6	3.5	0.4	43	0.2	8	30.5	9.5	110	4.3	470	14.5	1.7	11.5	1.3	380
363436	**Tunkillia**	1100	90		4.4	2.6	1.3	4.9	0.8	41	0.4	10	32	9.5	135	6	260	19.5	2.1	20.5	2.4	180
WGC165	**Tunkillia**	950	120		5.5	2.4	1.95	6.5	0.9	98	0.38	15	72	20.5	145	11	230	21	3.8	29	2.3	180
378933	**Tunkillia**	400	50		4.3	2.8	0.6	4.6	0.9	24	0.4	12	21	6	220	4.7	62	28.5	4.9	23	2.8	140
1840691	**Tunkillia**	1489	170	-1	0	0	1.58	0	0	89	0.42	13.2	53	0	124.4	0	315.4	13.8	0.9	32.4	3.15	396.6
370928	**Tunkillia**	600	21		1.8	1.4	0.5	1.6	0.4	12	0.2	12	7.5	2.3	155	1.5	66	14.5	1.7	10.5	1.6	170
370929	**Tunkillia**	250	110		3.8	2.1	0.6	3.8	0.6	50	0.3	8.5	42	11.5	250	6.5	40	33	3.1	16.5	2	100
370932	**Tunkillia**	700	115		4.6	2.5	1.2	4.4	0.8	68	0.4	11	46.5	12.5	185	7	94	23	3.2	20	2.5	220
370934	**Tunkillia**	500	66		2.5	1.5	0.7	3.1	0.5	44	0.3	10	23	7.5	200	4	105	28	3.1	11	1.6	190
370935	**Tunkillia**	220	35.5		1.3	1	0.4	1.3	0.3	22	0.3	14	10.5	3.7	260	1.6	56	25.5	4.9	7.5	1.5	80
370936	**Tunkillia**	200	52		1.6	1.3	0.4	1.7	0.4	29.5	0.3	14	14.5	5	240	2.2	110	30.5	5.5	11	1.9	90
444829	**Tunkillia**	1050	290		10	2.1	1.7	15	1.15	135	0.16	19	120	32	110	25.5	270	78	2.2	29.5	0.9	258
444830	**Tunkillia**	2450	165		1.4	0.7	2	3	0.2	105	0.1	3	54	16	72	5	550	12	0.4	5	0.6	249
879-47	**Tunkillia**	3650	160		2.3	1.1	2.3	3.6	0.41	90	0.2	7	58	18	39	6.5	750	13	0.7	12	1.1	310
444828	**Tunkillia**	900	135		4	2.1	1.4	4.4	0.67	80	0.3	11.5	54	15	140	8	165	21	2.3	17	2.1	128
444831	**Tunkillia**	500	10		0.91	0.55	0.72	0.55	0.16	6.5	0.09	3	4.2	1.15	40	0.67	900	3.3	0.64	3.9	0.65	76
879-29B	**Tunkillia**	800	86		0.7	0.3	1.4	1.75	0.11	48.5	0.05	4.5	32	9.5	15.5	3.6	600	13	0.46	3.1	0.25	160
444832	**Tunkillia**	290	68		2.5	1.2	0.8	2.5	0.4	36.5	0.1	8.5	27	7	74	4	92	3.1	1	10	0.7	306
444833	**Tunkillia**	1050	76		5.5	3.1	1.5	4.8	1	34	0.4	9.5	42.5	10	31.5	8	240	3.1	0.4	26	3.1	252
444834	**Tunkillia**	1100	210		8.5	3.7	2.3	9.5	1.4	125	0.4	15	92	24	35	15	340	7.5	0.7	31.5	2.7	176
444835	**Tunkillia**	290	130		6.5	4.1	0.8	6.5	1.3	66	0.6	20	48	15	220	8.5	58	37.5	6	33	4.4	80
387418	**Tunkillia**	958	75.7	12.2	3.85	2.12	1.116	4.65	0.73	35.5	0.3	12	29	7.91	201	5.27	308	15.7	3.36	21.5	2.03	182
387427	**Tunkillia**	929	92.5	5.22	4.32	2.44	1.722	5.87	0.86	43.2	0.39	12.1	39.2	10.3	135	6.9	849	12.6	4.11	23.8	2.44	166
387429	**Tunkillia**	882	39.2	4.17	1.36	0.78	0.547	1.93	0.27	19.7	0.13	4.5	14.9	4.12	120	2.17	291	9.2	1.76	8.1	0.86	91

Sample	Suite	Ba	Ce	Cs	Dy	Er	Eu	Gd	Ho	La	Lu	Nb	Nd	Pr	Rb	Sm	Sr	Th	U	Y	Yb	Zr
387431	**Tunkillia**	992	46.9	5.35	2.61	2.01	0.672	2.59	0.6	23.1	0.26	8.3	17.6	4.97	172	2.84	368	9.6	2.03	18.5	1.91	114
469565	**Tunkillia**	833	67.3	6.94	3.33	1.76	0.926	4.29	0.65	32.3	0.25	8.9	25.9	7.23	189	5.07	226	17.1	5.61	18.7	1.58	143
469566	**Tunkillia**	1447	50.3	5.02	3.33	2	0.692	3.04	0.68	24.5	0.21	10	18.3	5.23	185	2.93	357	9.8	4.28	16.9	1.61	146
469567	**Tunkillia**	793	103	6.03	4.02	2.03	1.426	5.9	0.76	49.3	0.29	12.1	40.3	10.9	218	6.77	148	20.3	3.22	20.3	1.79	235
469568	**Tunkillia**	1099	58	6.08	3.01	2.16	0.847	2.65	0.67	28.5	0.29	11.2	20.9	6.06	185	3.41	387	10.3	4.43	19.8	1.93	125
469569	**Tunkillia**	895	88.5	5.1	4.6	2.65	1.093	5.98	0.92	41.2	0.43	10.8	34.3	9.42	166	6.1	194	18	2.27	24.9	2.61	167
469570	**Tunkillia**	915	102	4.76	5.24	3.05	1.164	6.48	1.06	45.1	0.47	11.8	38.5	10.7	181	7.16	172	17.3	4.4	26.5	2.99	167
368571	**Tunkillia**	1000	38		1.6	0.8	1	2.3	0.3	20	0.1	6	15.5	4.6	100	2.7	370	10	1.6	7	0.8	250
368573	**Tunkillia**	1350	45		2	1.1	1.4	2.5	0.4	24.5	0.2	bdl	17.5	5.5	110	2.9	390	10.5	1.1	9	1.1	70
378920	**Tunkillia**	1000	45.5		1	0.6	0.9	1.5	0.2	28	0.1	18	15	4.9	150	2.3	440	20	2	4.7	0.6	70
378921	**Tunkillia**	210	33.5		1.1	0.7	0.5	1.5	0.2	18	0.1	6	12.5	3.8	135	2.2	155	30.5	1.6	5.5	0.8	120
378924	**Tunkillia**	1600	54		1.5	0.8	1.4	2.3	0.3	31	0.2	6	20	6	92	2.8	500	10	0.9	6.5	0.8	110
1840692	**Tunkillia**	862	169	1.83	0	0	1.06	0	0	92	0.25	10.2	65	0	122.7	0	57.4	14.1	1.2	24	2.04	258.3
1840702	**Tunkillia**	972	170	1.66	0	0	1.4	0	0	89	0.26	12.4	55	0	151	0	156.5	25.3	2.8	19.1	1.92	242.2
WGC81	**Tunkillia**	900	130		6.5	2.8	1.45	6	1.1	62	0.4	15.5	56	15	110	10	155	22	2.1	29	2.5	280
Christie1	**Tunkillia**	970	40	0	0	0	0	0	0	30	0	0	0	0	80	0	610	8	4	0	0	0
350435	**Tunkillia**	2750	60	4	3	2		3	0.5	32		15	23.5	7	120		340	4.5	1.5	14	2	180
370933	**Tunkillia**	150	80	-3	3.5	2	-0.5	4	0.5	38	-0.5	15	23.5	7	270	5	35	29	3.5	18	2	110
370937	**Tunkillia**	800	155	4	7.5	4	1	7	1.5	77	0.5	25	40	13	320	8.5	55	31	8	43	4	190
370938	**Tunkillia**	1150	180	-3	12	7	1	11	2.5	93	1	25	60	16	280	8	85	25	3.5	75	7	500
1948337	**Lzp1**	175.6	14.1	0.37	2.16	1.2	0.87	2.27	0.43	5.2	0.17	0.79	8.4	1.9	4.8	2.22	265.2	0.5	-0.05	12.4	1.07	38
1948338	**Lzp1**	183.7	8.8	0.28	1.56	0.88	0.7	1.58	0.31	3.6	0.08	0.37	5.6	1.29	4.4	1.5	278.7	0.31	-0.05	9.1	0.82	30
1948339	**Lzp1**	180	12	0.24	2.36	1.29	0.96	2.53	0.47	4.7	0.14	0.44	8.6	1.9	3.2	2.34	279.8	0.2	-0.05	13.1	1.11	30
1948341	**Lzp1**	200.3	13.8	0.38	2.34	1.27	0.97	2.43	0.47	5.6	0.14	0.54	9.1	1.99	4.6	2.38	278.6	0.29	-0.05	13.3	1.1	30
1948342	**Lzp1**	187.8	22.5	0.28	3.11	1.66	1.08	3.51	0.62	9.2	0.23	0.77	13.8	3.12	4.9	3.41	238.5	0.59	-0.05	17.4	1.5	52
1948343	**Lzp1**	183.5	14.4	0.29	2.6	1.44	0.95	2.82	0.51	5.6	0.16	0.37	10.2	2.19	4.6	2.64	245.5	0.23	-0.05	14.9	1.27	35
1948344	**Lzp1**	287.9	12.6	1.07	2.13	1.12	1	2.32	0.43	5.2	0.11	1.5	8.5	1.88	9.8	2.24	279.1	0.22	-0.05	12.4	1.01	30
1948345	**Lzp1**	360.1	14.9	8.06	1.31	0.7	1	1.53	0.25	7.1	0.06	0.7	7.6	1.87	58.6	1.58	454.4	0.38	-0.05	7.6	0.64	23

APPENDIX C: ISOTOPE DATA FROM REFERENCE SOURCES

Sm-Nd Isotope data from Payne et al. 2010 and unpubGSSAdata

Unit	Nd ppm	Sm ppm	143Nd/144Nd	Sm/Nd	147Sm/144Nd	143/144Nd CHUR*	143/144Nd DM*	T(DM)	T(CHUR)	εNd(0)	Age (t)	143/144Nd sample (T)	143/144 Nd sample	143/144Nd CHUR (T)	εNd (t) calc
Lzp1	14.1	3.4	0.511781	0.240544	0.1454	0.512638	0.51316	3.02364449	2.53598	-16.7248	1.74	0.510116	0.511781	0.510387	-5.30267
Lzp1	9.0	2.2	0.511831	0.242699	0.1467	0.512638	0.51316	2.96991463	2.450128	-15.7435	1.74	0.510152	0.511831	0.510387	-4.60922
Tunkillia	18.8	3.2	0.511752	0.170213	0.1042	0.512638	0.51316	1.93951035	1.459184	-17.2832	1.68	0.510601	0.511752	0.510466	2.641017
Tunkillia	57.5	9.7	0.511527	0.168696	0.1023	0.512638	0.51316	2.20939893	1.790931	-21.6722	1.68	0.510397	0.511527	0.510466	-1.35551
Tunkillia	33.6	5.7	0.511452	0.169643	0.1022	0.512638	0.51316	2.30806722	1.909066	-23.1352	1.68	0.510323	0.511452	0.510466	-2.80311
Tunkillia	20.1	4.3	0.511875	0.213930	0.1302	0.512638	0.51316	2.31317571	1.74701	-14.8838	1.68	0.510437	0.511875	0.510466	-0.57648
Tunkillia	45	6.7	0.511372	0.148889	0.0899	0.512638	0.51316	2.1785832	1.803548	-24.6958	1.68	0.510379	0.511372	0.510466	-1.70828
Tunkillia	13.5	1.9	0.511366	0.140741	0.0863	0.512638	0.51316	2.12488548	1.753241	-24.8128	1.68	0.510413	0.511366	0.510466	-1.04669
Tunkillia	57.5	6.9	0.511001	0.120000	0.0729	0.512638	0.51316	2.31377755	2.010219	-31.9329	1.68	0.510196	0.511001	0.510466	-5.29691
Tunkillia	27.1	3.9	0.511111	0.143911	0.0873	0.512638	0.51316	2.44344427	2.121412	-29.7871	1.68	0.510147	0.511111	0.510466	-6.25855
Tunkillia	39.2	7.2	0.511414	0.183673	0.1115	0.512638	0.51316	2.57024215	2.183582	-23.8765	1.68	0.510182	0.511414	0.510466	-5.56029
Tunkillia	84.6	13.8	0.511271	0.163121	0.0988	0.512638	0.51316	2.47627821	2.122434	-26.666	1.68	0.510179	0.511271	0.510466	-5.61305
Tunkillia	44	7.3	0.511459	0.165909	0.0997	0.512638	0.51316	2.24898666	1.849198	-22.9987	1.68	0.510358	0.511459	0.510466	-2.12492
Tunkillia	17.6	3.1	0.511568	0.176136	0.1046	0.512638	0.51316	2.19907921	1.768092	-20.8724	1.68	0.510412	0.511568	0.510466	-1.0501
Tunkillia	17	2.9	0.511483	0.170588	0.1026	0.512638	0.51316	2.27452686	1.867333	-22.5305	1.68	0.510349	0.511483	0.510466	-2.2824
Tunkillia	26	3.8	0.511433	0.146154	0.0888	0.512638	0.51316	2.0864734	1.699709	-23.5059	1.68	0.510452	0.511433	0.510466	-0.27522
Tunkillia	55.9	9.5	0.511281	0.169946	0.1026	0.512638	0.51316	2.54623166	2.191584	-26.4709	1.68	0.510147	0.511281	0.510466	-6.23957
Tunkillia	25.4	3.9	0.511382	0.153543	0.0922	0.512638	0.51316	2.20693538	1.828572	-24.5007	1.68	0.510363	0.511382	0.510466	-2.01016
Tunkillia	59.2	11.6	0.511811	0.195946	0.118	0.512638	0.51316	2.12270118	1.600407	-16.1322	1.68	0.510507	0.511811	0.510466	0.810154
Tunkillia	53.8	9.1	0.511494	0.169145	0.1025	0.512638	0.51316	2.2577144	1.847702	-22.3159	1.68	0.510362	0.511494	0.510466	-2.04526
Tunkillia	23.5	4.2	0.511376	0.178723	0.108	0.512638	0.51316	2.54012541	2.162584	-24.6178	1.68	0.510183	0.511376	0.510466	-5.54722